measurement systems laboratory

massachusetts institute of technology, cambridge, massachusetts 02139

RE-90

STUDIES OF ORBITAL EÖTVÖS EXPERIMENTS

BY

PHILIP K. CHAPMAN

JUNE 30, 1977

MASSACHUSETTS INSTITUTE OF TECHNOLOGY
DEPARTMENT OF AERONAUTICS AND ASTRONAUTICS
MEASUREMENT SYSTEMS LABORATORY
CAMBRIDGE, MASSACHUSETTS 02139

RE-90
FINAL REPORT

STUDIES OF ORBITAL EÖTVÖS EXPERIMENTS

BY

PHILIP K. CHAPMAN

CONTRACT NGR22-009-735

SUBMITTED TO
NATIONAL AERONAUTICS AND SPACE ADMINISTRATION
WASHINGTON, D.C.

JUNE 30, 1977

ABSTRACT

The advent of the space shuttle (STS) will make it possible to carry out relativistic experiments in a laboratory in free fall. One of the most important such experiments, because it is essential to the foundations of general relativity, is the test of the universality of the ratio of passive gravitational to inertial mass for bodies, which is known as the Eötvös experiment. This report presents analyses of a direct force-balance technique for carrying out this experiment in space, which is intended to give sufficient sensitivity to allow investigation of the gravitational interactions of energy stored in the weak interaction. It is found that a sufficiently sensitive experiment may be possible in which the apparatus is allowed to float in the payload bay of the shuttle, although maximum sensitivity requires a fully autonomous, free-flying experiment.

The heart of this experiment is an exceedingly sensitive dual accelerometer, containing two proof masses constructed of the materials whose Eötvös ratio is to be compared. It is hoped to use an electrostatically-suspended accelerometer for this application; but it is impossible to test such an accelerometer in a terrestrial laboratory if electrostatic forces are used to support the proof mass, because of cross-coupling between the support and sensitive axes. For use in development of the accelerometer, a magnetic microbalance is proposed in which the weight of the proof mass is supported by magnetic forces which vary very slowly with the proof mass position. It may then be possible to build an electrostatic suspension to control the proof mass with electrode spacings, voltages, etc., similar to those which are needed in free fall. It is shown that at least two different mechanizations of the magnetic suspension may be feasible.

TABLE OF CONTENTS

TABLE OF CONTENTS (continued)

LIST OF FIGURES

CHAPTER ONE

THE EÖTOVÖS EXPERIMENT

I.1 Introduction

In Newtonian gravitational theory, the force acting on a particle of inertial mass m_1, due to the gravitational field of another particle of mass M_2 is given by

$$\underline{F} = m_1\ddot{\underline{r}} = - GM_1M_2r^{-3}\underline{r} \qquad [1]$$

where G is the gravitational constant, $\underline{r}$ is the position vector of the particle relative to the source of the field and M_1 is the gravitational mass of the particle. As has been noted by Bondi[1], three logically distinct concepts of mass occur in this equation: (i) inertial mass m_1, which determines the acceleration of the particle under a given force; (ii) passive gravitational mass M_1, which determines the force on the particle in a given gravitational field; and (iii) active gravitational mass M_2, which determines the strength of the gravitational field generated by a particle. The equivalence of active and passive gravitational mass is a consequence of the law of action-reaction [which is not a Lorentz-invariant concept, so that it must be handled with care in relativistic generalizations of the theory],

but the universality of gravitational phenomena depends on the separate assumption that the Eötvös ratio

$$k = M/m \qquad [2]$$

is a constant for all bodies (at least, for all bodies which are so small that gravity-gradient effects in the external gravitational field are unimportant). The value of G is normally so chosen that this ratio is unity.

The hypothesis that k is independent of the chemical composition or internal structure of a sufficiently small body is a statement of the Weak Principle of Equivalence, which is an axiom in general relativity and in most other theories of gravitation, although in some (for example, the Brans-Dicke cosmology[2]) the ratio is allowed to vary from point to point in spacetime. It should be noted that the Weak Principle is necessary but not sufficient for the validity of general relativity (and especially for its geometric interpretation in terms of the metric of spacetime); the theory developed by Einstein requires the Strong Principle of Equivalence, which states that no self-contained physical measurement, carried out in an infinitesimal region of spacetime, can distinguish between gravitation and a suitably chosen inertial acceleration. As a corollary, a free-fall coordinate system, if sufficiently limited in extent, is physically absolutely equivalent to an inertial frame (local Lorentz frame).

The Strong Principle is subject to direct experimental proof only if it is believed that it is presently possible to enumerate every feasible type of physical measurement. However, it is possible that the Weak Principle implies the Strong Principle, a suggestion known as the Schiff Conjecture[3] which has, as yet, been satisfactorily demonstrated only for restricted cases.[4] If it can be proven, the Weak Principle will become the primary foundation of gravitational theory.

The Weak Principle of Equivalence is obviously supported by the common observation that all bodies fall with the same acceleration under gravitation (as in the famous and perhaps apocryphal test by Galileo at the Leaning Tower in Pisa). This phenomenon was demonstrated dramatically on television by David Scott on Apollo 15, when he dropped a feather and a hammer together to the lunar surface. Accurate evidence for the validity of the principle however consists of experiments of the Eötvös type, whose distinguishing characteristic is that they are null measurements, taking advantage of some situation in which there is a nominal balance between inertial and gravitational forces in order to achieve quite remarkable precision. Given two bodies, of materials A and B, these experiments may be regarded as measurements of the Eötvös number

$$\eta(A,B) = k(A) - K(B) \qquad [2A]$$

Eötvös himself used the fact that, in a horizontal plane determined by a plumb bob, there is (in the northern hemisphere) a small southward component of centrifugal acceleration, due to the diurnal rotation of the Earth, and an equal but opposite component of gravitation. The magnitude of these horizontal accelerations reaches a maximum of about 1.7 cm/sec^2 at 45^o latitude. A torsion pendulum was constructed in which bobs of different materials were attached to opposite ends of an arm which was suspended by a fiber at its balance point. If η for the two bobs differed from zero, a small torque would be produced about the vertical, which would affect the rest orientation of the arm relative to the laboratory. Because this Eötvös torque was a sinusoidal function of the azimuth angle of the arm, the arm orientation would not then change by exactly 180^o when the fiber suspension was rotated through precisely that angle. In a series of painstaking experiments between 1889 and 1922, Eötvös showed[5] that, for a variety of pairs of materials, η differs from zero by at most a few parts in 10^9.

In 1962, Dicke et al[6] built an improved torsion balance, which possessed triangular symmetry to reduce the effects of local gravity gradients and which was designed to take advantage of the balance which exists between the gravitational pull of the sun and the centrifugal force due to the motion of the Earth in its orbit. The accelerations involved here were somewhat smaller (c. 0.6cm/sec^2) than in the experiments of Eötvös, but they were modulated with a

24-hour period by the rotation of the Earth, allowing frequency discrimination against some interfering torques and, more importantly, eliminating the need to disturb the system by rotating the suspension relative to the laboratory. The accuracy achieved was about one part in 10^{11}, in a comparison of gold and aluminum test masses.

Using a modified form of the Dicke experiment, Braginski[7] in 1972 improved the accuracy further, by about one order of magnitude.

As discussed in Chapter II, the advent of space technology has opened up opportunities for Eötvös experiments of unprecedented accuracy.

I.2 Possible Violations of the Equivalence Principle

General relativity is a theory of gravitation which is self-consistent, complete, and in agreement with all experiments to date. Moreover, it is compellingly elegant, in a way unmatched by any other theory which has been proposed. Even if other gravitational theories are to be considered, there are strong arguments[8] that the only viable theories are metric theories -- i.e., theories in which spacetime possesses a metric which satisfies the Equivalence Principle by exhibiting locally Lorentz frames. The best confirmation of the Equivalence Principle (and especially of the Strong Principle) lies in the nature of the theories to which it leads, rather than in the direct experimental evidence for it. Nevertheless,

an unsatisfactory aspect of metric theories of gravitation is that, despite much effort which has gone into unified field theories, gravitation remains conceptually quite distinct from the other fields of physics, being regarded as an expression of the curvature of spacetime. Furthermore, as will be shown, there are difficulties with the Equivalence Principle itself which suggest that anomalies might be revealed by continued experimentation.

In designing such tests, a theoretical framework would obviously be useful which predicted where violations might be found. It is not reasonable to discuss tests of the Equivalence Principle in terms of a theory which assumes its validity. What is needed is a gravitational theory which starts with minimal assumptions (e.g., Lorentz covariance and reduction to Newtonian theory in that limit), identifies clearly the additional assumptions which lead to a metric theory, and then systematically explores the consequences of changing those assumptions. The spin-two field theory of gravitation[9,10], which leads to general relativity when non-linear terms due to the energy density of the gravitational field itself are included, may provide a model for such a development.[11]

In the absence of a comprehensive theory, the best that can be done is to consider some isolated possible anomalies.

I.2.1 Differences in Composition: The Weak Interaction

The classical Eötvös experiment is a test of the possibility that the ratio of passive to inert mass of a body depends on its

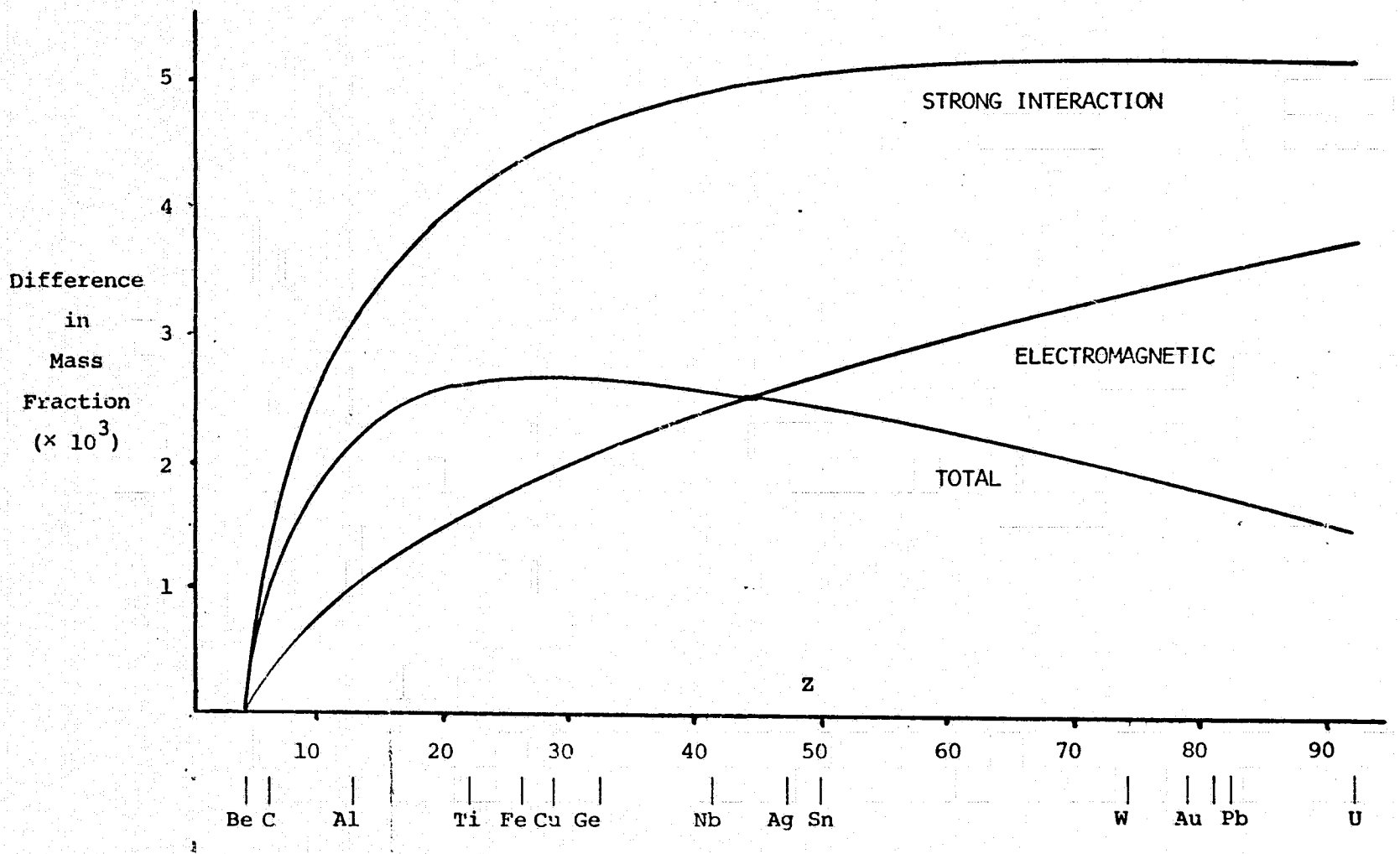

Figure I: Binding Energy Mass Fractions

chemical composition. In more fundamental terms, the hypothesis to be tested is that one or more of the forms of energy which make up matter exhibits an anomalous value of this ratio. Examination of this hypothesis will show the motivation for further improvements in the accuracy of the experiment, as well as providing some important design considerations.

Ordinary matter may be regarded as consisting of energy stored in a combination of the following forms:

(i) The elementary particles (both real and virtual) which make up atoms, particularly protons, neutrons and electrons.

(ii) The strong interaction, which binds protons and neutrons together to form nucleii.

(iii) The electromagnetic interaction, which binds electrons and nucleii together to make atoms, atoms together to make molecules and crystal lattices, and which weakens the strong attraction of protons in a nucleus.

(iv) The weak interaction, which is responsible for β-decay processes.

(v) The gravitational interaction, which holds stars together and binds planets and stars into solar systems and solar systems into galaxies, but which is very weak indeed on the laboratory scale.

Eötvös experiments using bodies of widely different composition allow conclusions to be drawn concerning the passive mass of some of these forms of energy (excluding the gravitational interaction, which is discussed in Section I.2.2). Energy conservation requires conservation of passive mass in reversible transformations between forms of energy, since otherwise it would in principle be possible to convert a system to its heavy form, extract energy by lowering

it in a gravitational field, and then lift it after conversion back to its light form, allowing a perpetual motion machine. However, this does not prohibit equal and opposite changes in passive mass amongst components of such transformations, so that anomalous results of the Eötvös experiment are possible.

In order to estimate the accuracy required in such experiments, assume for simplicity that only the i^{th} form of energy exhibits an Eötvös anomaly, with k_i the ratio of passive to inert mass. If $\alpha_i(A)$ is the fractional contribution of this energy to the overall inert mass-energy of body A, Eq. (2A) reads

$$\eta(A,B) = (1 - k_i)\ [\alpha_i(B) - \alpha_i(A)] \qquad [3]$$

Since the mass fractions of the different energy forms add to unity for a given body, the difference in the particle mass fractions for two bodies is equal, apart from sign, to the difference in the binding energy mass fractions. Figure I shows the difference between the total binding energy for an element of atomic number Z and that of beryllium, which is arbitrarily chosen as a reference. This curve, which is obtained from the semi-empirical mass formula of Weizsacker[12], may be useful in designing tests of the hypothesis that particles, of whatever type, exhibit an anomalous Eötvös ratio. For example, it is clear that this anomaly, if it exists, would be maximized in a test which compared beryllium with copper or iron. Such a choice would in fact give a test 6 times as sensitive as one using gold and aluminum, with no other changes in the experimental conditions.

The total binding energy is made up basically of the electromagnetic and strong interaction energies, the latter being negative since it is an attractive force between nucleons. The weak and gravitational interactions are negligible by comparison. The electromagnetic and strong components of the difference in binding energy of an element of atomic number Z and that of beryllium are also shown in Fig. I, where it is seen that the optimum choice for test of the hypothesis that one of these energies has an anomalous Eötvös ratio is beryllium and an element of high atomic number, such as gold or uranium. The achievable improvement over gold and aluminum is by a factor of 2.4 for the strong interaction, but only by about 50% for the electromagnetic interaction.

The shape of the curves in Fig. I suggest that an Eötvös experiment in which beryllium is used as a standard for comparison with both copper and gold would give optimum sensitivity for each of the three above forms of energy -- and if an anomaly were detected, it would be possible to determine, from the relative magnitude of the results for copper and gold, which energy was responsible.

The Dicke test, showing that $\eta(\mathrm{Au,Al}) < 10^{-11}$, allows the following conclusions to be drawn from Fig. I:

$k_{\mathrm{particles}}$ is less than 2×10^{-8}

k_{strong} is less than 5×10^{-9}

$k_{\mathrm{electromagnetic}}$ is less than 6×10^{-9}

Note that this simple analysis applies to particles only when they are considered as a group. Drawing conclusions from the Eötvös experiment about the passive mass of particular types of particles (e.g., neutrons) requires a more detailed analysis, as the differences in mass fractions are not necessarily given with sufficient accuracy by the semi-empirical mass formula and, in any case, depend on the particular isotopic composition of the samples tested. An analysis by Schiff[13] suggests that Eötvös experiments to date have demonstrated with convincing precision that protons, neutrons and electrons (and their antiparticles) do not exhibit anomalous gravitational behavior.

Energy stored in the nucleus by virtue of the weak interaction is typically of order 10^7 times less than that due to the strong interaction[14]; in other words, weak interaction energy may contribute a fraction of order one part in 10^9 to the mass of an atom. In view of the uncertainties in this calculation, and of the fact that only differences in the mass fraction between different materials contribute in an Eötvös experiment, it is clear that such experiments to date are insufficient to allow any statement about the passive mass of weak energy. On the other hand, the Eötvös experiment in orbit which is discussed in Chapter II, which is intended to have a sensitivity of about one part in 10^{14}, is fully capable of detecting any substantial violation of the Equivalence Principle by weak energy. It is this possibility which provides the strongest motivation for the Eötvös experiment in space.

I.2.2 The Gravitational Self-Energy

For an approximately spherical body of radius r, the fractional contribution of the energy in its gravitational field to the overall inert mass is of order

$$\alpha_g = \frac{Gm}{rc^2} \qquad [4]$$

where c is the speed of light. This number is of order 10^{-25} for laboratory bodies, much too small to be of any experimental interest, but it is of order 10^{-9} for the Earth and 10^{-6} for the Sun, so that solar system experiments are much more promising.

As was pointed out originally by Nordtvedt[15], a differential acceleration towards the Sun of the Earth and Moon would result if gravitational self-energy lacked passive mass. The resulting polarization of the lunar orbit about the Earth is detectable by lunar laser ranging using the retroreflectors left on the Moon during the Apollo program. Results to date indicate no anomaly, the accuracy in the measurement of the Eötvös ratio of gravitational energy being about 2%[16].

If this effect existed, the Earth would exhibit an anomalous acceleration towards the sun of order 10^{-12}g. While this could in principle be detected by a sensitive accelerometer in a laboratory, difficulties with first- and second-order solar gravity gradients, tidal effects, seismic noise, etc., probably preclude such an experiment.

It would be quite surprising if this type of Eötvös anomaly were discovered. One third of the anomalous precession of the perihelion of Mercury can be construed as arising from the active mass of energy stored in the solar gravitational field[10] (there is more spherically symmetric mass inside the planet's position at aphelion than at perihelion). Moreover, if the passive mass of a gravitating system changes when gravitational energy is converted to other forms (e.g., kinetic), it is clearly possible to conceive gedanken experiments which would exhibit small violations of energy conservation.

A somewhat similar effect can arise in those theories which, while obeying the Equivalence Principle, allow spatial variations in the gravitational constant (e.g., the Brans-Dicke theory[2]). Because the gravitational self-energy depends on G, spatial gradients of G can produce small anomalous forces on a massive body[17].

I.2.3 Spin-Orbit Interactions

It is predicted by general relativity[18] that a spinning body does not follow exactly a geodesic in the Riemannian space-time determined by neighboring bodies, when it is in acted on by no forces. In other words, a gyroscope in a gravitational field experiences an anomalous acceleration, which has been calculated by Schiff[19] for the case of a spherically symmetric, static field as

$$\underline{a}_s = \frac{3GM}{mc^2 r^5}[(\underline{r}\cdot\underline{H})(\underline{r} \times \underline{v}) + (\underline{r}\cdot\underline{v})(\underline{r} \times \underline{H})] \qquad [5]$$

where M is the mass of the source of the field, m is the mass of the gyro, $\underline{r}$ is the radius vector to the gyro, $\underline{H}$ is its angular momentum, and $\underline{v}$ is the orbital velocity. For a circular orbit, for which $\underline{r}\cdot\underline{v} = 0$, with $\underline{H}$ lying in the plane of the orbit, an Eötvös experiment which compared the gyro with a non-spinning body would reveal an Eötvös ratio which varied sinusoidally at orbital period, of amplitude

$$\eta_S = \frac{3H\Omega}{mc^2} \qquad [6]$$

where Ω is the orbital angular velocity. For example, a large gyro in low Earth orbit, with a wheel radius of one meter, spinning at 10,000 rpm (close to the value at which centrifugal stresses would tear it apart), would exhibit an Eötvös ratio of order 10^{-17}. Careful design and a sufficiently large apparatus might make this effect experimentally detectable, thereby providing another test of general relativity. Although such a device would, in principle, be capable of detecting the difference between an inertial acceleration and a gravitational field, this would not necessarily violate the Strong Principle of Equivalence, which is limited to infinitesimal regions. A spinning body cannot be infinitesimal, even in principle, essentially because the periphery must move at less than the speed of light. Thus this experiment would constitute a test of the consequences, and not the foundations of general relativity.

I.2.4 The Electromagnetic Radiation Reaction

At first sight, radiation from an accelerated charged particle seems to violate the Equivalence Principle. How does a charged body, at rest in a terrestrial laboratory, know that it is experiencing a gravitational field and not an acceleration, so that it does not radiate? The usual answer to this, of somewhat dubious validity, is that radiation phenomena must occur over distances of at least a wavelength, and hence cannot be considered as an experiment in an infinitesimal region. In any case, it is of interest to calculate the anomalous Eötvös ratio which would be expected if a charged body were compared with an uncharged one in Earth orbit, because of the radiation reaction.

The power radiated by an accelerated charged particle is given by the Larmor formula[20]

$$P = - m\tau\dot{v}^2 = \underline{F}_{rad}\cdot\underline{v} \qquad [7]$$

where

$$\tau = \frac{2}{3}\frac{e^2}{mc^3} \qquad [8]$$

where e is the charge. In a circular orbit,

$$\dot{v}^2 = (\underline{v} \times \underline{\Omega})^2 = v^2\Omega^2 \qquad [9]$$

so that [7] may be written

$$[\underline{F}_{rad} = m\tau\Omega^2\underline{v}]\cdot\underline{v} = 0 \qquad [10]$$

or

$$\underline{F}_{rad} = m\tau\Omega^2(\underline{R} \times \underline{\Omega}) = - m\underline{g} \times \tau\underline{\Omega}$$

where $\underline{R}$ is the radius of the orbit. The radiation reaction force is thus a drag, opposite to the orbital velocity, whose magnitude is less than the weight of the particle by the factor $\tau\Omega$. The characteristic time τ has its maximum value, 6.26×10^{-24} seconds, in the case of an electron, which, in low Earth orbit, would thus exhibit an Eötvös ratio of at most about 10^{-26}. The effect is therefore negligible.

CHAPTER TWO

AN EÖTVÖS EXPERIMENT IN ORBIT

II.1 Basic Considerations for a Space Experiment

As discussed in the previous Chapter, there is now good evidence that all the forms of energy which make up matter obey the Equivalence Principle, with the possible exception of energy stored in the weak interaction. It appears that this last form of energy can be checked by carrying out an Eötvös experiment with a sensitivity improved by several orders of magnitude, to about one part in 10^{14}.

The advent of space technology has made possible a substantial improvement in the experimental conditions for the Eötvös experiment. In low Earth orbit, there exists a balance between gravitational and centrifugal accelerations whose magnitude is close to one gee. This is to be compared with the forces available to Eötvös[5] (1.7 milligee) and Dicke et al[6,7] (0.6 milligee). Moreover, the free-fall environment in orbit allows great reduction in the problems associated with suspension of the apparatus, such as coupling to ambient noise. In principle, then, the Eötvös signal can be increased by three orders of magnitude, and the noise level substantially reduced. In view of the importance of the experiment to the

foundations of general relativity, it is an obvious candidate for performance in space. As discussed in Section III.3, it may be an ideal experiment in terms of making use of the capabilities of the Space Transportation System (space shuttle), in the development of the apparatus as well as in performance of the final experiment.

The most obvious technique for carrying out this experiment in orbit is to use an adaptation of the rotational balances which have been successful in terrestrial experiments. However, gravity-gradient torques may swamp those due to Eötvös forces unless great care is taken to make the system inertially symmetrical. Without going into the details of the design of such a balance, some general conclusions may be drawn.

For simplicity, consider a system with one of its principal axes along the orbit normal. The gravity-gradient torque is then along the orbit normal and of magnitude (calculated in Section III.2.4).

$$T_g = -\frac{3}{2}\Omega^2 \Delta I \sin 2\theta \qquad [12]$$

where ΔI is the difference in the moments of inertia about the principal axes which lie in the orbit plane and θ is the angle between one of these axes and the local vertical.

Let us suppose the system is constructed of two different materials, A and B, for which the ratios of passive to inert mass are k(A) and k(B), respectively. The Eötvös torque about

the center of mass is then

$$\underline{T}_e = - \underline{g} \times [k(A) \int_A \underline{r}\, dm + k(B) \int_B \underline{r}\, dm]$$

$$= - n\underline{g} \times [\int_B \underline{r}\, dm]$$

$$= - \eta m\, \underline{g} \times \underline{a} \qquad [13]$$

where $\underline{g}$ is the local gravitational field, $\underline{r}$ is the radius vector from the CM of the system to an element of mass dm, and

$$\underline{a} = \frac{1}{m} \int_B \underline{r}\, dm \qquad [14]$$

With appropriate symmetry, $\underline{a}$ will lie in the orbit plane, but generally not along one of the principal axes. $\underline{T}_e$ is then along the orbit normal and of magnitude

$$T_e = - \eta m g a \sin \phi \qquad [15]$$

where ϕ is the angle between $\underline{a}$ and the local vertical. In order to estimate the difficulty of inertially balancing the system, a reasonable condition to impose is that the frequency of gravity-gradient oscillations be less than that due to Eötvös torques. If I is the moment of inertia about the axis along the orbit normal and b the radius of gyration about this axis, this condition may be written, using [12] and [15], as

$$\frac{\Delta I}{I} < \frac{\eta a R}{3b^2} \qquad [16]$$

where R is the radius of the orbit. For a given system geometry, the gravity-gradient torques increase faster with the size of the system than do the Eötvös torques, so relatively small apparatus is required to allow adequate inertial balancing. For $a \simeq b \simeq 10$ cm, [16] requires

$$\frac{\Delta I}{I} < 2 \times 10^{-7} \qquad [17]$$

in order to achieve an accuracy of $\eta \simeq 10^{-14}$. Inertial balancing to this accuracy is difficult but not impossible with current technology, especially as it may be possible to exploit the double-angle dependence of [12] and a design difference in the directions of $\underline{\alpha}$ and a principal axis to effect final balancing on orbit.

Even if this condition can be met, it must be recognized that the torques under consideration are extraordinarily weak. From [15], the angular frequency of oscillation due to the Eötvös torques is given by

$$\omega_e^2 = \frac{\eta a R}{b^2} \Omega^2 \qquad [18]$$

which, under the conditions assumed in [17], gives a period of some 2000 hours! It is clear that very great care indeed would be required to protect the balance from non-gravitational disturbing torques, such as those due to the Earth's magnetic field, radiation pressure or perhaps residual atmospheric drag.

Furthermore, it is highly desirable to design an experiment from which the data can be extracted more quickly.

II.2 Force-Balance Techniques

In order to overcome the difficulty of inertially balancing an Eötvös torque-measurement apparatus for use in free fall, an alternative technique is under study in the M.I.T. Measurement Systems Laboratory[21,2] (and also at the Hansen Laboratories of Physics, Stanford University[23]), in which the Eötvös forces are to be measured directly, without converting them into torques. The design was motivated by the following considerations:

i) Gravity-gradient forces may be minimized by placing the centers of mass of the bodies to be compared as nearly as possible at the same point in space.

ii) The tensor properties of residual gravity-gradient forces may be used to distinguish them from the phenomenon under study.

iii) The Eötvös force may be modulated by rotating the apparatus, allowing operation at higher frequencies and minimizing the duration of the experiment.

iv) The design allows resonance to be used to enhance the sensitivity to Eötvös forces.

v) Force-measuring devices (accelerometers) are simpler to instrument than torque-measuring devices, which must include gyros and/or star-trackers.

vi) While a force-measurement experiment may seem, at first sight, more subject to disturbances due to external forces (magnetic, residual aerodynamic, etc.) than a torque balance might be, in fact the force balance technique allows discrimination against these effects in a way which is difficult or impossible with a torque balance. In any case, if necessary these forces can be reduced or eliminated by well-established "pure gravity orbit" techniques.[24]

As sketched in Fig. II, the proposed apparatus is a satellite which consists basically of an aluminum wheel, spinning about its axis of symmetry, which is nominally aligned normal to the plane of the orbit. This orientation is, of course, stable under gravity-gradient torques. A sensitive electrostatic accelerometer is mounted radially in the plane of the wheel; it consists of a cylindrical electrode structure with an internal test mass constructed of material A and an external, annular test mass constructed of material B, as sketched in Fig. III. The accelerometer is so designed that, when the two test masses are at their null positions, their centers of mass are nominally coincident with each other and with the center of mass (CM) of the satellite. The object of the experiment is, of course, to compare the Eötvös ratios of materials A and B, by a differential measurement of the forces which they experience as the satellite moves along its orbital path.

II.3 Analysis of the Experiment: Ideal Case

Let m, M be the inert and passive masses of test mass A and m', M' those of test mass B. The null positions are taken accurately coincident with the CM of the system and the displacements of the test masses from null are denoted by x, x' respectively. The mass of the wheel is assumed to be so large that motion of the test masses does not appreciably shift the position of the CM within the system. The satellite moves in a perfectly circular orbit about the Earth, which is taken to be spherically symmetric, and

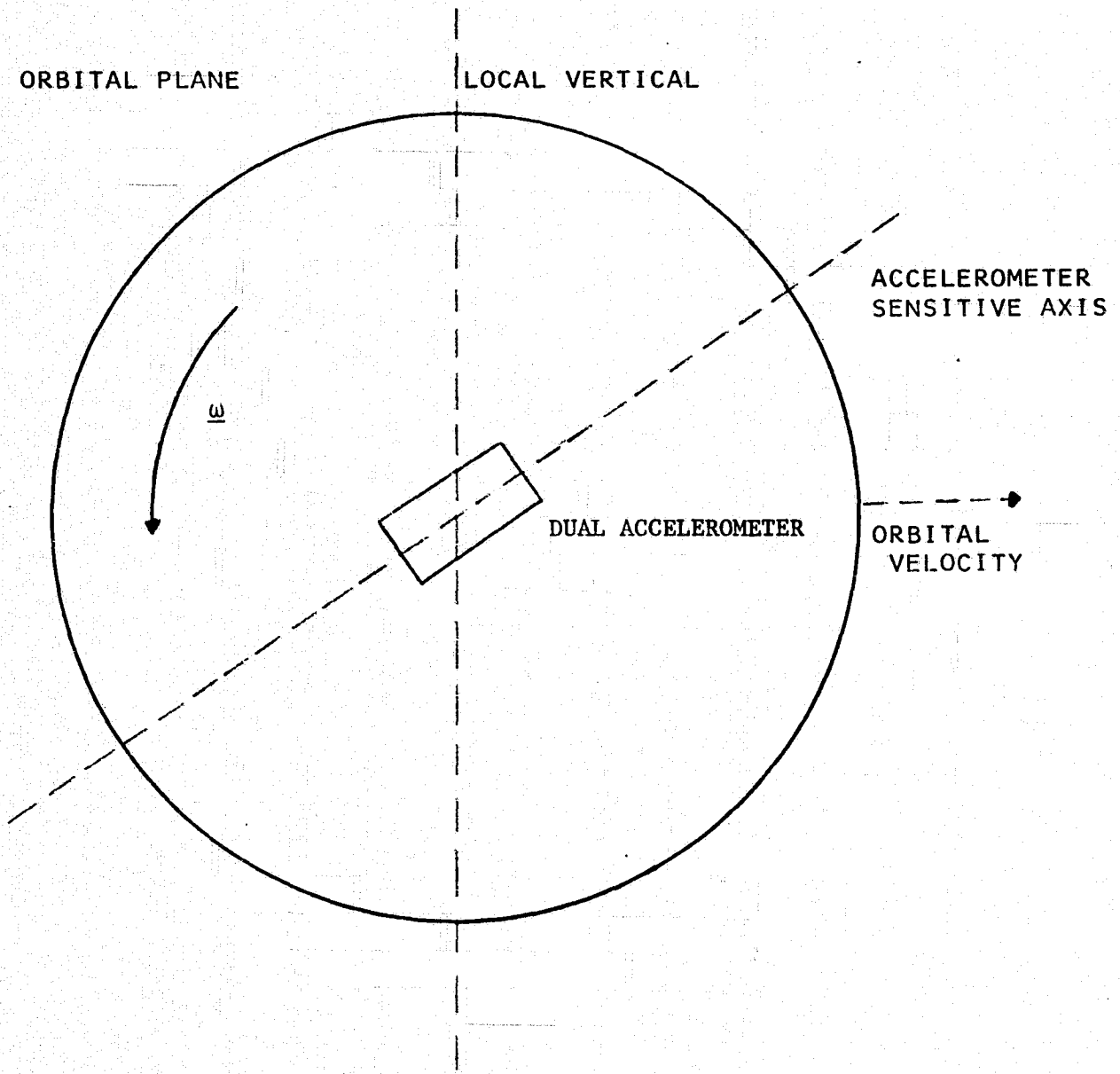

Fig. II.: ORBITAL EÖTVÖS EXPERIMENT

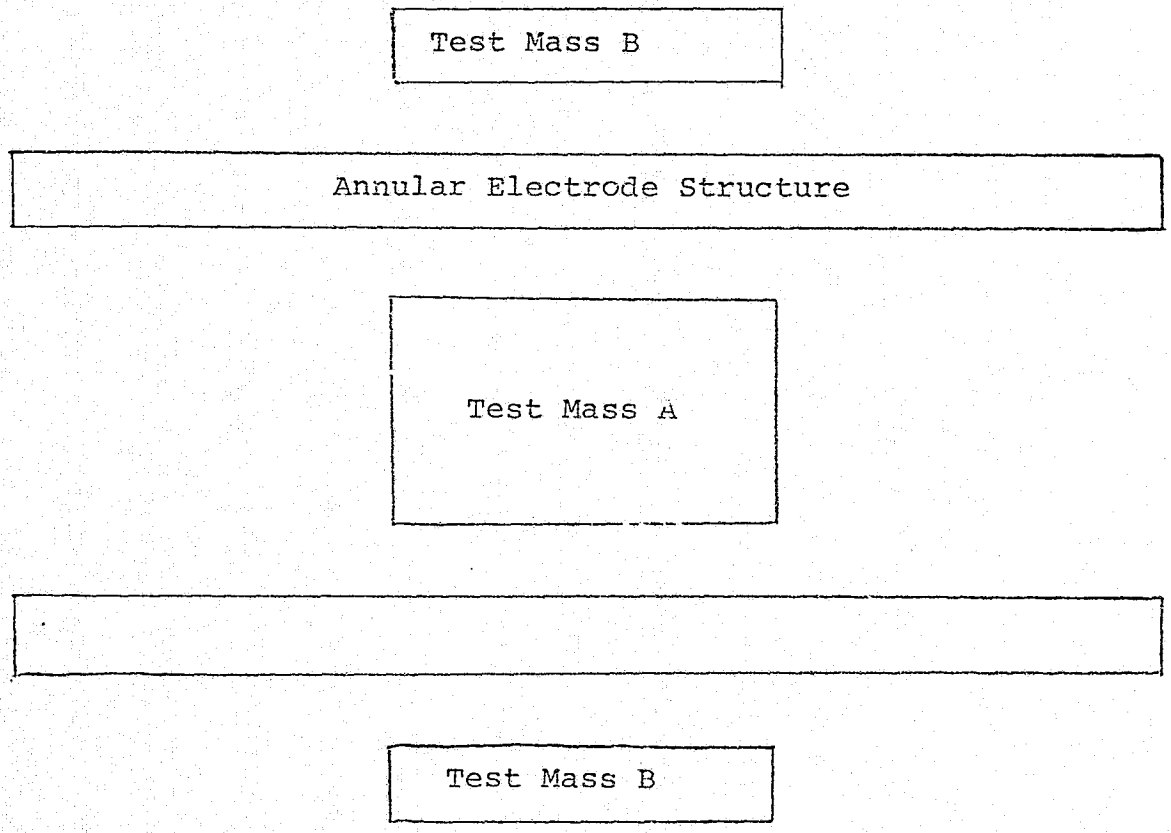

Figure III. Dual Accelerometer

no external forces other than gravitation act on the system. Ideally, the equation of motion of test mass A is then

$$m\ddot{x} = -mq + m\omega^2 x + [M\underline{g} - m\underline{g}^*].\underline{i}_x \qquad [19]$$

where ω is the inertial angular velocity of the wheel, q is a servo restraint force applied to the test mass, $\underline{i}_x$ is a unit vector along the (common) accelerometer axis, $\underline{g}$ is the gravitational field at the test mass and $\underline{g}^*$ is the inertial acceleration of the CM of the system, due to terrestrial gravitation. In this equation, forces which are perpendicular to the sensitive axis, such as the Coriolis term, have been dropped: the cross-coupling between support and sensitive axes of the accelerometer is assumed zero.

A similar equation to [19], using appropriately primed quantities, applies to test mass B.

Without loss of generality, the Eötvös ratio of the satellite as a whole may be taken as unity. This is equivalent to defining the gravitational constant as that measured in a Cavendish experiment using masses of the same average composition as the system. Then

$$\underline{g}^* = -\Omega^2 \underline{R} \qquad [20]$$

where Ω is the orbital angular velocity of the satellite and $\underline{R}$ is the geocentric position vector of its CM.

The gravitational field may be expanded in a Taylor series about the CM, most conveniently in tensor notation. For future

reference, we write the field for a general position r_i (i = 1,2,3) relative to the CM and compute the second-order terms, although only the first-order gravity gradients are required at present. For test mass A,

$$Mg_i - mg_i^* = m[kg_i - g_i^*]$$

$$= m[(k-1)g_i^* + kr_j[\frac{\partial g_i}{\partial R_j}]^* + \frac{k}{2!} r_j r_k [\frac{\partial^2 g_i}{\partial R_j \partial R_k}]^* + \ldots] \qquad [21]$$

where k = M/m and * means the quantity is to be computed at the CM. Since k is very close to unity (as demonstrated by terrestrial Eötvös experiments), it may be taken as such in [21], except in the first term, so that

$$Mg_i - mg_i^* = m[(k-1)g_i^* + \Gamma_{ij} r_j + T_{ijk} r_j r_k + \ldots] \qquad [22]$$

here the first- and second-order gravity gradient tensors are given by the partial derivatives of the terrestrial gravitational field as

$$\Gamma_{ij} = [\frac{\partial g_i}{\partial R_j}]^* = \frac{\partial}{\partial R_j}[-GM_\oplus R^{-3} R_i]^*$$

$$= -\Omega^2[\delta_{ij} - 3R^{-2} R_i R_j] \qquad [23]$$

and

$$T_{ijk} = \frac{1}{2}[\frac{\partial^2 g_i}{\partial R_j \partial R_k}]^*$$

$$= \frac{3}{2}\Omega^2 R^{-2}[R_i \delta_{jk} + R_j \delta_{ik} + R_k \delta_{ij} - 5R^{-2} R_i R_j R_k] \qquad [24]$$

where $M_\oplus$ is the mass of the Earth and δ_{ij} is the unit tensor.

Substituting the first-order terms in [19] yields

$$\ddot{x} + q - [\omega^2 - \Omega^2 + 3\Omega^2 R^{-2}(\underline{R}.\underline{i}_x)^2]x = (k-1)\underline{g}^*\underline{i}_x \qquad [25]$$

or, since $\underline{i}_x$ is rotating with respect to the local vertical (i.e., $\underline{R}$) with an angular velocity $(\omega-\Omega)$,

$$\ddot{x} + q - [\omega^2 + \tfrac{1}{2}\Omega^2 + \tfrac{3}{2}\Omega^2 \cos 2(\omega-\Omega)t]x = (k-1)g \cos (\omega-\Omega)t \qquad [26]$$

If q is a simple spring restraint,

$$q = Kx \qquad [27]$$

this is recognized as a standard Mathieu equation, driven by sinusoidal forcing function proportional to the difference between the Eötvös ratio for test mass A and that for the whole system.

By writing out the equation similar to [26] for test mass B, using primed quantities, and subtracting from [26], we obtain

$$\ddot{y} + \Delta q - [\omega^2 + \tfrac{1}{2}\Omega^2 + \tfrac{3}{2}\Omega^2 \cos 2(\omega-\Omega)t]y = \eta g \cos (\omega-\Omega)t \qquad [28]$$

where $y = x-x'$, $\Delta q = -q'$, and $\eta = k - k'$ is the Eötvös number for materials A and B. A Mathieu equation for the differential motion of the two test masses results if q' is also a spring restraint with the same spring constant per unit mass as q.

The ideal performance equation [28] demonstrates the possibility of carrying out an Eötvös experiment with apparatus of this type. It would, of course, be possible to use an accelerometer with a single test mass, made of the material to be tested against the satellite as a whole, according to [26]. The advantages of the dual accelerometer are:

i) Any pairs of materials may be compared, merely by changing proof masses. This flexibility may be used to enhance accuracy in the search for violations of equivalence by different forms of energy, as discussed in the previous chapter.

ii) More importantly, as shown in the next Chapter, the configuration allows discrimination against many disturbing forces, which do not appear in the ideal equation [26].

It is to be noted that the amplitude of the Eötvös acceleration in [28] is ηg. In designing a force-balance Eötvös experiment with an accuracy of one part in 10^{14}, a prerequisite is an accelerometer with a sensitivity (to sinusoidal acceleration) of $10^{-14}g$. The problem of designing and, most importantly, testing such an accelerometer is taken up in Chapter IV.

CHAPTER THREE

SATELLITE SYSTEM DESIGN

III.1 Preliminary Stability Analysis

In beginning a more detailed design of the force-balance satellite experiment discussed in the last Chapter, the first question to be taken up is that of determining the conditions under which Eq. [28] (or Eq. [26]) has stable solutions. To this end, we assume a servo restraint force between the test masses of the form

$$\Delta q = Ky + 2\lambda\dot{y} \qquad [29]$$

which represents a simple spring, with damping. The equation of differential motion [28] is then

$$\ddot{y} + 2\lambda\dot{y} + [W^2 - \tfrac{3}{2}\Omega^2 \cos 2(\omega-\Omega)t]y = \eta g \cos (\omega-\Omega)t \qquad [30]$$

where

$$W^2 = K - \omega^2 - \tfrac{1}{2}\Omega^2$$

For resonance, one might first choose $\lambda = 0$ and

$$W^2 = (\omega-\Omega)^2 \qquad [31]$$

but unfortunately this ideal, infinite-Q case results in divergent solutions of the Mathieu equation[25]. The degree of damping required for stability may be calculated by the techniques described in Ref. 23. We consider the homogeneous version of [30] and, to put it in a standard form, first write

$$\tau = (\omega-\Omega)t \qquad [32]$$

which yields (with $\frac{dy}{d\tau}$ now denoted by $\dot{y}$, etc.)

$$\ddot{y} + \frac{2\lambda}{(\omega-\Omega)}\dot{y} + \frac{1}{(\omega-\Omega)^2}[W^2 - \frac{3}{2}\Omega^2 \cos 2\tau]y = 0 \qquad [33]$$

The substitution

$$y = e^{-\lambda\tau/(\omega-\Omega)}z(\tau) \qquad [34]$$

reduces this equation to the standard form

$$\ddot{z} + (a - 2b \cos 2\tau)z = 0 \qquad [35]$$

with

$$a = (W^2 - \lambda^2)/(\omega-\Omega)^2 \qquad [36]$$

and

$$b = \frac{3}{4}\Omega^2/(\omega-\Omega)^2 \qquad [37]$$

If [35] has stable solutions, then [33] certainly does also; but, because of the damping factor in [34], it is possible for [33] to be stable even though $z(\tau)$ is divergent. We must therefore

investigate the properties of the unstable solutions of [35], for different values of a & b. The stability diagram is Fig. 8 of Ref. 25: the relevant region of the a-b plane, for operation near resonance ($a \simeq 1$) is shown in Fig. IV. The curves separating stable from unstable regions are given by[26]

$$a^* = 1 + b - \frac{1}{8}b^2 - \frac{1}{64}b^3 - \frac{1}{1536}b^4 + \ldots \qquad [38a]$$

and

$$a\dagger = 1 - b - \frac{1}{8}b^2 + \frac{1}{64}b^3 - \frac{1}{1536}b^4 - \ldots \qquad [38b]$$

If the point (a,b) lies on the curve [38a], the solution of [35] is periodic and even in τ. If it lies on [38b], it is periodic and odd in τ. Between these curves, the solution is divergent; it may be written in the form[27]

$$z(\tau) = Ae^{\mu\tau} \sum_{k=-\infty}^{k=\infty} c_k e^{2jk\tau} + Be^{-\mu\tau} \sum_{k=-\infty}^{k=\infty} c_k e^{-2jk\tau} \qquad [39]$$

where the summations represent periodic functions, A & B are constants determined by the initial conditions, and μ is a function of a & b. It is clear from [34] that the solutions to the original equation [30] will be stable if

$$\lambda > (\omega-\Omega)|\mu| = \lambda_{min} \qquad [40]$$

Between the curves [38a] and [38b], we may choose a parameter σ such that[27]

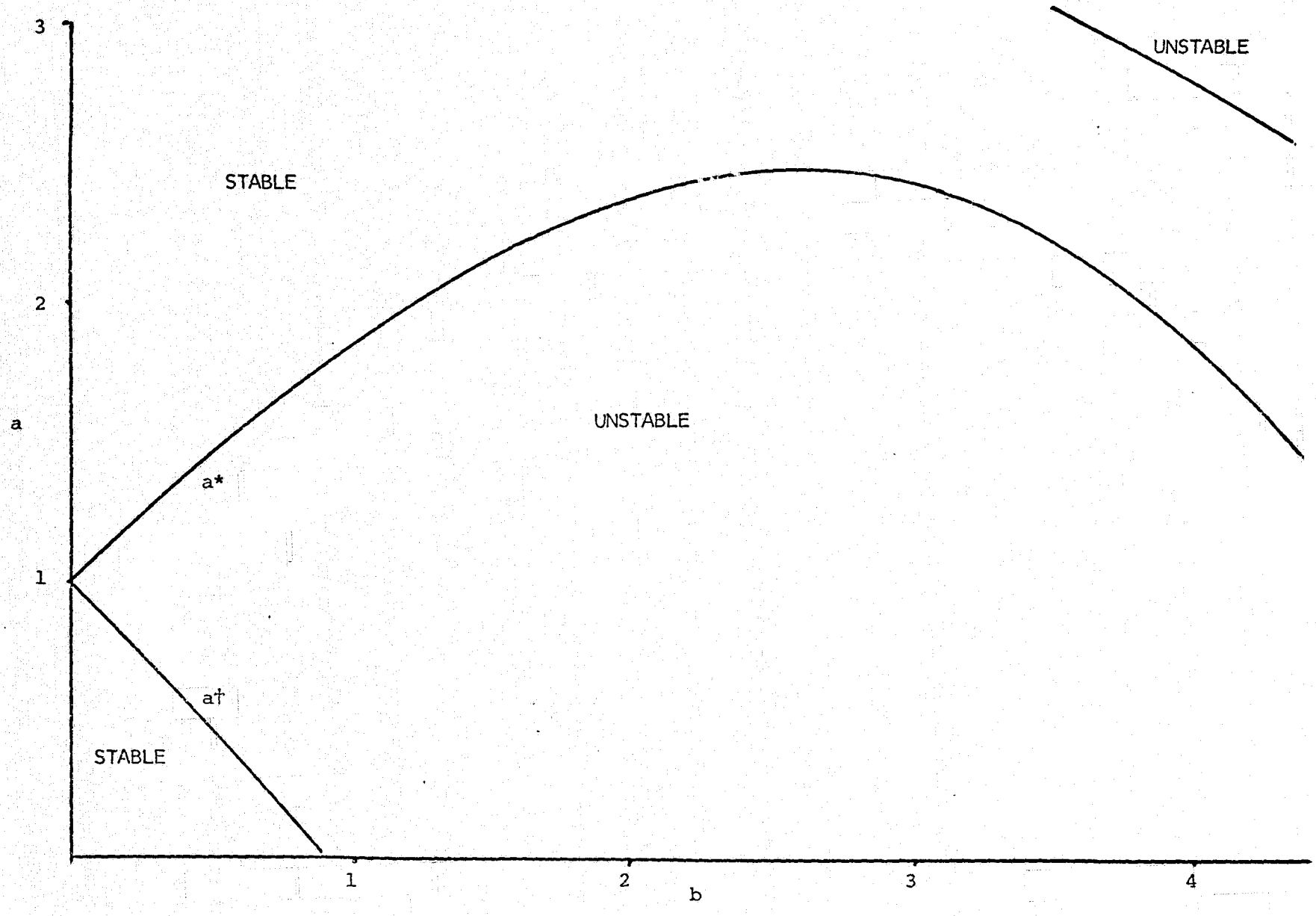

Figure IV: Stability Boundaries for the Standard Mathieu Equation

$$a = 1 - b\cos 2\sigma + \frac{1}{4}b^2(\frac{1}{2}\cos 4\sigma - 1) + \frac{1}{64}b^3\cos 2\sigma$$

$$+ \frac{1}{16}b^4(\frac{1}{3} - \frac{11}{32}\cos 4\sigma) - \ldots \qquad [41]$$

which reduces to [38b] for $\sigma = 0$ and to [38a] for $\sigma = \pi/2$. Given values of a & b, [41] may be solved numerically for σ and then[25]

$$\mu = -\frac{1}{2}b\sin 2\sigma + \frac{3}{128}b^3\sin 2\sigma - \frac{3}{1024}b^4\sin 4\sigma - \ldots \qquad [42]$$

We consider two modes of operation of the system which might be used in practice:

i) $\omega >> \Omega$

If the wheel is spinning at an angular velocity much larger than orbital angular velocity, [37] shows $b<<1$. It is then sufficient to retain only up to the quadratic terms in b in [41]. To estimate the required damping, we assume operation at resonance ($a = 1$), and then [41] becomes

$$\frac{1}{4}b^2(\frac{1}{2}\cos 4\sigma - 1) - b\cos 2\sigma \simeq 0$$

or

$$\cos^2 2\sigma - \frac{4}{b}\cos 2\sigma - \frac{3}{2} \simeq 0 \qquad [43]$$

which may be solved to yield, to second order in b,

$$\cos 2\sigma \simeq -\frac{3}{8}b \qquad [44]$$

To this accuracy, [42] then gives

$$\mu \simeq -\frac{1}{2}b \qquad [45]$$

and, from [40], the minimum damping for stability is

$$\lambda_{min} = \frac{1}{2}(\omega-\Omega)b = \frac{3}{8}\frac{\Omega^2}{(\omega-\Omega)} \qquad [46]$$

Under these conditions, the time-varying coefficient in [30] produces a small perturbation to a simple second-order harmonic system, which, according to [46], has

$$Q_{max} = \frac{(\omega-\Omega)}{2\lambda_{min}} = \frac{1}{2|\mu|} = \frac{1}{b} = \frac{4}{3}\left(\frac{\omega}{\Omega}-1\right)^2 \qquad [47]$$

It is thus clear that very light damping may be used if ω is high enough. For example, in low orbit, with ω = 10 rpm, a value $Q_{max} \simeq 10^6$ is obtained.

If the solution [39] is substituted in [34] and τ replaced by t, by [32], it is easily seen that the effective damping factor is

$$\lambda_{eff} = \lambda - (\omega-\Omega)|\mu| \qquad [48]$$

so that

$$Q_{eff} = \frac{(\omega-\Omega)}{2\lambda_{eff}} \qquad [49]$$

can be much higher than Q_{max} if λ is close to λ_{min}. Comparison with an accurate numerical calculation shows that [46] is an adequate expression for λ_{min} if ω is greater than about 3Ω.

ii) $\omega = 0$ (Inertially stationary wheel).

In this case, from [37], $b = \frac{3}{4}$. If we put $\lambda = \lambda_{min}$ and use the resonant condition [31] in [36], we find, using [40],

$$a = 1 - \mu^2 \qquad [50]$$

Since we cannot be assured a priori that μ is small, this expression must be used in [41] and the equation solved simultaneously with [42]. An iterative numerical procedure (reguli falsi) gives

$$\lambda = .365\ \Omega \qquad [51]$$

Note that the expression [46] gives a result which is accurate within about 3% even in this extreme case. While high effective Q can still be achieved in principle, in the presence of the heavy damping implied by [51], in such a case small changes in the damping could lead to instabilities. This is one of the reasons the spinning system is preferred for this experiment.

In practice, of course, a simple spring with damping is a very elementary servo. A more realistic design requires study of disturbing forces acting on the system, and the question of system stability must be examined again in the light of this analysis. For example, it would be possible to compute and apply a correction for the time-varying coefficient in [30], if this should prove desirable. However, [46] provides a good rule of thumb for estimating the minimum allowable damping in the absence of such compensation.

III.2 Disturbing Forces

In the system under consideration the Eötvös acceleration, if it exists, always lies along the local vertical, and is modulated by rotation of the wheel. Any forces applied to the wheel or to the test masses which appear, in a reference frame attached to the wheel, at frequencies close to $(\omega-\Omega)$, the angular velocity of the wheel with respect to a local vertical reference frame, may masquerade as Eötvös forces, although considerable discrimination is possible when the differential motion of the two test masses is regarded as the output of the system. Limits to this filtering action of the dual accelerometer will be considered below, but, to maximize sensitivity, it is clearly desirable to minimize extraneous forces, in particular those, such as residual atmospheric drag, which are approximately constant in the orbital frame. Those forces which have constant components along the local vertical may prove especially troublesome.

Techniques exist[28] for isolating the system from most external forces, by making it "drag-free". Indeed, it was the availability of such techniques which provided one motivation for designing the system to measure Eötvös forces directly. However, only those forces which, directly or indirectly, appear along the sensitive axis of the accelerometer are of interest, and this may allow a simpler mechanization than that involved in forcing the entire satellite to follow a pure gravity orbit. This possibility of course depends on the feasibility of designing an accelerometer

with sufficiently low cross-coupling between the support and sensitive axes.

The list of possible disturbances which must be taken into account includes at least the following effects:

1. The orbit of the satellite is slightly elliptical.
2. The center of mass of the system does not coincide with the center of gravity.
3. The system moves in the vicinity of a massive object, which exerts gravity-gradient forces on it (for example, the experiment is free-flying in the shuttle payload bay).
4. The wheel angular momentum is not along a principal axis, nor along the normal to the orbit plane.
5. The null positions of the test masses do not coincide with each other, nor with the CM of the system.
6. The sensitive axes of the dual accelerometer are not coincident, nor are they perpendicular to the spin axis of the wheel.
7. Support forces for the test masses couple into the sensitive axes, due to Coriolis effects as well as to mechanical and electromagnetic imperfections.
8. The CM of the system shifts when the test masses move.
9. The test masses are affected by stray electromagnetic forces, generated by the satellite or arising from natural ambient fields.
10. Various mechanical forces (noise) are applied to the wheel.
11. The displacement detector is noisy, exerts forces on the test masses, and possibly exhibits non-linearities (e.g., threshold).

System design for this experiment is not yet complete, and not all of these effects have as yet been taken into account.

III.2.1 Orbit Eccentricity

If the orbit is not precisely circular, the first-order gravity-gradient tensor [23] must be written

$$\Gamma_{ij} = - GM_{\oplus}R^{-3}[\delta_{ij} - 3j_ij_j] \qquad [52]$$

where j_i is a unit vector along the local vertical, to allow for variations in the orbit radius R. The equation of motion [25] of the first test mass is then

$$\ddot{x} + q - [\omega^2 - GM_{\oplus}R^{-3}(1 - 3(\underline{j}.\underline{i}_x)^2]x = (k-1)GM\ R^{-2}\underline{j}.\underline{i}_x \qquad [53]$$

If we assume for simplicity that the accelerometer sensitive axis is along the local vertical at perigee, then

$$\underline{j}.\underline{i}_x = \cos\ (\omega t - \phi) \qquad [54]$$

where ϕ is the true anomaly, the instantaneous geocentric angle away from perigee in the orbit. The radius of the orbit is given by[29]

$$R = \frac{p}{1 + e\ \cos\ \phi} \qquad [55]$$

where e is the eccentricity and p is the semi-latus rectum, which is the radius of the orbit when the true anomaly is 90°.

In order to find the variation of ϕ with time, we first introduce a new variable E, called the eccentric anomaly, by the relation

$$\tan\frac{\phi}{2} = \left(\frac{1+e}{1-e}\right)^{1/2} \tan\frac{E}{2} \qquad [56]$$

The eccentric anomaly is the solution of Kepler's equation[29]

$$E - e \sin E = \Omega_o t \qquad [57]$$

where Ω_o is the mean orbital angular velocity. This equation may be solved in terms of a Fourier-Bessel series expansion for E, but, to first order in e, the solution is obviously

$$E \simeq \Omega_o t + e \sin \Omega_o t \qquad [58]$$

If we write

$$\phi = \Omega_o t + \delta \qquad [59]$$

and insert this and [58] in [56], we find, after some reduction, to first order in δ and e,

$$\delta = 2e \sin \Omega_o t \qquad [60]$$

and then [54] gives

$$\underline{j}\cdot\underline{i}_x = \cos(\omega-\Omega_o)t + 2e \sin \Omega_o t \sin(\omega-\Omega_o)t \qquad [61]$$

Now, to first order,

$$GM_\oplus R^{-3}(1 - 3(\underline{j}\cdot\underline{i}_x)^2) = \Omega_o^2(1 + 3e \cos \Omega_o t)[1 - 3\cos^2(\omega-\Omega_o)t$$

$$- 12e \cos(\omega-\Omega_o)t \sin \Omega_o t \sin(\omega-\Omega_o)t$$

$$= \Omega_o^2[-\frac{1}{2} - \frac{3}{2}\cos 2(\omega-\Omega_o)t$$

$$+ 3e[-\frac{1}{2}\cos \Omega_o t - \frac{7}{4}\cos(2\omega - 3\Omega_o)t + \frac{1}{4}\cos(2\omega-\Omega_o)t]] \qquad [62]$$

and, on the right side of [53],

$$GM_{\oplus}R^{-2}\underline{j}.\underline{i}_x = g_o(1 + 2e\cos\Omega_o t)(\cos(\omega-\Omega_o)t + 2e\sin\Omega_o t\sin(\omega-\Omega_o)t)$$

$$= g_o[\cos(\omega-\Omega_o)t + 2e\cos(\omega-2\Omega_o)t] \qquad [63]$$

Suppose now that there is a steady state offset Δy_o between the null positions of the two test masses. When the equation of differential motion is formed, analogously to [28], by subtracting from [53] a similar equation for the other test mass, the first order effects of the orbit eccentricity will be, firstly, to change slightly the time-varying coefficient, according to [62]; and, secondly and more importantly, to introduce a driving force which, apart from constant terms, is given by

$$f = \Omega_o^2\Delta y_o[\tfrac{3}{2}\cos 2(\omega-\Omega_o)t + 3e(\tfrac{1}{2}\cos\Omega_o t + \tfrac{7}{4}\cos(2\omega-3\Omega_o)t$$

$$- \tfrac{1}{4}\cos(2\omega-\Omega_o)t)] \qquad [64]$$

Note that there is no component of this force with the principal frequency $(\omega-\Omega)$ at which the Eötvös acceleration appears. In fact, the double harmonic term (independent of the eccentricity) can be used to drive the null positions of the two test masses into coincidence.

If the wheel is inertially stationary, however, a term

$$f_1 = \tfrac{3}{4}\Omega_o^2 e\,\Delta y_o\cos\Omega_o t \qquad [65]$$

appears in [64], at the same frequency Ω_o exhibited by the Eötvös acceleration in this case. Since the amplitude of the Eötvös signal is $\eta g = \eta\Omega_o^2 R_o$, we must have

$$\Delta y_o << \frac{4\eta R}{3e} o \qquad [66]$$

if f_1 is not to be falsely interpreted. For $e \simeq .002$, a reasonable value for low Earth orbit, and if the design sensitivity is $\eta = 10^{-14}$, the null offset must be small compared to 40 microns. This is not a difficult requirement, but the effect could become troublesome if it were desired to attempt much greater sensitivity. In any case, the problem can be avoided by operation in the spinning mode.

III.2.2 CM-CG Deviations

Consider an arbitrary rigid body in circular orbit. Set up a reference frame with origin at the center of the Earth, rotating at orbital angular velocity so as to keep the 1-axis along the orbit normal and the 3-axis along the local vertical. In this frame, the total (gravitational plus centrifugal) force acting on an element of mass dm in the body, located at a position vector r_i with respect to the CM, is (cf. Eqs. [23] and [24]).

$$dF_i = -\Omega^2(R_i + r_i)dm + g_i^* dm + \Gamma_{ij} r_j dm + T_{ijk} r_j r_k dm + \ldots \qquad [67]$$

where R_i is the geocentric position vector of the CM and g_i^* is now the gravitational field at the CM. By definition of the CM,

$$\int r_i dm = 0 \qquad [68]$$

so that integration of [67] over the body yields

$$F_i = m(g_i^* - \Omega^2 R_i) + T_{ijk} \int r_j r_k dm + \ldots \qquad [69]$$

The definition of the inertia tensor of the body is[30]

$$I_{jk} = \int (r_n r_n \delta_{jk} - r_j r_k) dm \qquad [70]$$

so that the last term in [69] may be written

$$\Delta F_i = T_{ijk}\delta_{jk} \int r_n r_n dm - T_{ijk} I_{jk}$$

$$= - T_{ijk} I_{jk}$$

$$= - \tfrac{3}{2}\Omega^2 R^{-2} [R_i I_{jj} + 2R_j I_{ij} - 5R^{-2} R_i R_j R_k I_{jk}] \qquad [71]$$

since, from [24]

$$T_{ijk}\delta_{jk} = T_{ijj} = \tfrac{3}{2}\Omega^2 R^{-2} [3R_i + R_i + R_i - 5R_i] = 0 \qquad [72]$$

Now let us suppose that the principal 1-axis of the body lies along the orbit normal, and that the principal 3-axis makes an angle θ with the local vertical. In the principal-axis frame, I_{jk} is of course diagonal, and

$$R_i = R[0, \sin\theta, \cos\theta] \qquad [73]$$

$$R_j I_{ij} = R[0, I_2 \sin\theta, I_3 \cos\theta] \qquad [74]$$

and

$$R_j R_k I_{jk} = (I_2 \sin^2\theta + I_3 \cos^2\theta) R^2 \qquad [75]$$

so that [71] may be written, after some trigonometric reduction, as

$$\Delta \underline{F} = -\frac{3}{2} m g R^{-2} \begin{vmatrix} 0 \\ (\xi_1^2 - \frac{3}{4}\xi_2^2 - \frac{1}{4}\xi_3^2)\sin\theta + \frac{5}{4}(\xi_2^2 - \xi_3^2)\sin 3\theta \\ (\xi_1^2 - \frac{1}{4}\xi_2^2 - \frac{3}{4}\xi_3^2)\cos\theta + \frac{5}{4}(\xi_2^2 - \xi_3^2)\cos 3\theta \end{vmatrix} \qquad [76]$$

where ξ_1, ξ_2, ξ_3 are the radii of gyration. Compared to an infinitesimal body, a finite-sized body in orbit thus, in general, experiences a small additional gravitational acceleration. We note first that, if $\theta = 0$, the incremental acceleration is along the local vertical, and of magnitude

$$\varepsilon = -\frac{3}{2} g R^{-2} (\xi_1^2 + \xi_2^2 - 2\xi_3^2) \qquad [77]$$

If $\xi_2^2 = \xi_3^2$ as in the case of a wheel spinning about the normal to the orbit, then, as is to be expected, [76] shows that the acceleration is along the local vertical, regardless of θ. If the wheel is taken as a uniform disc of radius a, then [77] gives

$$\underline{\varepsilon} = \frac{3}{8}\left(\frac{a}{R}\right)^2 \underline{g} \qquad [78]$$

For low Earth orbit ($R \simeq 6550$ km) and $a \simeq 50$ cm,

$$\varepsilon = 2 \times 10^{-15} g \qquad [79]$$

The test masses are physically much smaller, so the acceleration applied to them is expected to be at least two orders of magnitude smaller than [79], depending on their design. Thus [78] appears in the system exactly like an Eötvös acceleration, as if the ratio of passive to inertial mass of the wheel were greater than unity, except that it is sensed by both test masses. The filtering capability thus provided should permit, as far as this effect is concerned, operation down to about $\eta = 10^{-17}$. At this level, it becomes necessary to take into account the differences in the detailed inertial properties of the two test masses -- specifically, the difference obtained when [76] is applied to each of them.

The effect [79] could perhaps be reduced by an order of magnitude by making the entire apparatus as small as possible. A better technique would be to make the "wheel" isoinertial, as [76] and [77] vanish if the radii of gyration are all equal. In this case, however, the system would not be positively stable in its nominal attitude under gravity-gradient torques, and a separate attitude control system would be required.

Of course, it is not necessary that the system be isoinertial in order for [77] to vanish. If we choose

$$\xi_1 = 2\xi_3^2 - \xi_2^2 \qquad [80]$$

then it is easy to see that the principal 1-axis will have maximum moment of inertia, as desired for attitude stability, as

long as $\xi_3^2 > \xi_2^2$. These conditions are met, for example, by a flat rectangular plate, lying in the plane of the orbit with its long dimension horizontal, if the length-to-width ratio is $\sqrt{2}$:1. However, the fact that the acceleration vanishes for particular orientations of particular asymmetric bodies is academic, since it is necessary to rotate the apparatus* to modulate the Eötvös forces. What is significant is the component of [76] along the sensitive axis of the accelerometer, with $\theta = (\omega-\Omega)t$. If, for example, the accelerometer is along the principal 2-axis, it would be desirable to have

$$\xi_1^2 = \frac{3}{4}\,\xi_2^2 + \frac{1}{4}\,\xi_3^2 \qquad [81]$$

since the third-harmonic term may be filtered out. From this, however, the condition $\xi_1^2 > \xi_3^2$ implies $\xi_2^2 > \xi_3^2$, whereas $\xi_1^2 > \xi_2^2$ implies $\xi_3^2 > \xi_2^2$. Thus [81] is incompatible with ξ_1^2 being the maximum radius of gyration: the best that can be achieved is inertial symmetry.

III.2.3 Nearby Massive Bodies

For a preliminary evaluation of the feasibility of operating the experiment in the vicinity of other equipment (e.g., free-flying in the payload bay of the space shuttle), we consider here the gravitational effects on the system of a body of mass M°, located at a vector position $\underline{R}^\circ$ with respect to the CM of the system. For numerical estimates, we take M° = 1 ton, R° = 2 meters.

*The apparatus is, of course, rotating relative to the orbital frame even in the inertially stationary case.

At the CM of the apparatus, the gravitational field of this object is of order 10^{-9}g. The presence of the body thus makes a negligible change in the Eötvös signal (the right-hand side of [28]). The direct effect of this field, the acceleration of the apparatus towards the body, is also negligible, being two orders of magnitude smaller than the apparent relative accelerations due to the terrestrial gravity gradient.

The first-order gravity gradients due to the disturbing body can be more significant, changing the time-varying coefficient in [28]. Close to the surface of a spherical body of density ρ, the gravity gradient tensor will have components of order

$$GMR^{-3} \simeq \frac{4}{3}\pi G\rho \qquad [82]$$

and thus can be comparable with the terrestrial gravity gradients if the density is comparable to that of the Earth. We can in fact write [28] as

$$\ddot{y} + \Delta q - [\omega^2 + \tfrac{1}{2}GM_\oplus R^{-3}(1 + 3\cos 2(\omega-\Omega)t) + \tfrac{1}{2}GM^\circ R^{\circ -3}(1 + 3\cos(\omega t - \theta))]y = \eta g \cos(\omega-\Omega) \qquad [83]$$

where θ is the angle between $\underline{R}^\circ$ and an inertial reference direction and it has been assumed for simplicity that $\underline{R}^\circ$ lies in the plane of the orbit. If $\underline{R}^\circ.\underline{R}$ is constant (e.g., if the shuttle is stabilized with respect to the local vertical), the time dependence

of the disturbing gravity gradients will be the same (apart from a phase angle) as that of the terrestrial term. In this case, the principal effect is an increase in the coefficient b in [35]; by [47], this may increase somewhat the damping required for stability.

With the numerical values for M° and R° given above, the disturbing gravity gradients are two orders of magnitude smaller than the terrestrial term. The conclusion is thus that, if it is desired to operate the experiment in the shuttle, a more careful study of the effects of first-order vehicle gravity gradients is warranted, but it appears probable that the sensitivity of the experiment will not be compromised by this effect.

Further difficulties arise when the second-order gradients are considered. If $\underline{R}°$ is in the plane of the wheel, whose radius is a, then the acceleration of the wheel towards M°, due to the difference in position of the CG and the CM, is given by [78] as

$$\underline{\varepsilon} = \frac{3}{8}a^2GM°R^{-4} \simeq 4 \times 10^{-11}g \qquad [84]$$

with the numerical values and a = 50 cm. Comparison with [79] shows the effect is three orders of magnitude larger than that due to the second-order terrestrial gradients.

The acceleration [84] is, of course, extraordinarily small by ordinary standards. If the experimental apparatus has a mass of 100 kg, for example, the force exerted on it due to this effect

is only 4 millidynes; this is equal to the radiation pressure exerted by reflection of a light beam whose power is 6 watts!

It is not possible to avoid the effect [84] by attaching the experimental apparatus in a suitable bearing to the structure of the vehicle (even if the mechanical noise problems thereby introduced could be overcome), because the test masses would then sense the direct gravitational field of the disturbing mass ($\sim 10^{-9}$g) as well as terrestrial gravity gradients ($\sim 10^{-7}$g if the attachment point is 2 meters from the CM of the shuttle). Free flight is essential.

The acceleration ε is similar to an Eötvös acceleration but of course does not represent a limit to the accuracy of the experiment if carried out in a large vehicle in orbit. In the first place, the effect is sensed equally by both test masses; the discrimination afforded by the differential measurement depends on the design of the dual accelerometer, but is expected to be several orders of magnitude. Further discrimination is possible if the vector $\underline{R}°$ varies in direction or magnitude, with frequency components different to those involved in the Eötvös measurement. For example, a slow rotation of the shuttle would remove the acceleration ε from the passband of the accelerometer. In order to avoid the essentially continuous thrusting which this might involve if the experiment were not quite close to the CM of the vehicle, a possible technique would be to align the roll axis of the shuttle approximately along the local vertical and allow it to execute dumbbell gravity gradient

oscillations, of an amplitude sufficiently small so that the apparatus does not strike the walls of the payload bay. In this case, there would be a constant component of ε, but measurement of the component at the dumbbell frequency (in the sum motion of the test masses) would allow computation and subtraction of it in data processing.

More Herculean measures are possible to counteract this effect. For example, measurement of the acceleration, as discussed above, would provide the data needed to exert a compensating force on the apparatus (perhaps by radiation pressure!). Alternatively, it is in principle possible to add compensating masses, attached to the shuttle, around the apparatus, in such a way as to reduce the second-order gravity gradients.

Without going to such lengths, it is probably possible to carry out the experiment in the shuttle payload bay, with an accuracy of perhaps one part in 10^{14}*. If higher accuracy is required, launching the apparatus as an independent satellite is probably the preferred technique, paying the price for the increased autonomy which would then be needed.

*At this level, it may be necessary to take into account second-order gravity-gradient forces on the test masses themselves.

III.2.4 Attitude Motions of the Apparatus

a) Torque-free Nutation

To start with the simplest possible case, we assume that the system is inertially symmetric about the spin axis, having a moment of inertia I_s about that axis and I_t about transverse axes, and that the test masses are so small that their motion does not affect the motion of the system as a whole. The motion is then that of a classical rigid body. For future reference, we start by sketching the well-known derivation of the nutation frequency, in the absence of gravity-gradient or other torques[31].

The equation of motion is determined by conservation of angular momentum:

$$[\dot{\underline{H}}]_I = [\dot{\underline{H}}]_B + \underline{\omega} \times \underline{H} = 0 \qquad [85]$$

where $[\dot{\underline{H}}]_I$ is the rate of change of angular momentum relative to inertial space;

$[\dot{\underline{H}}]_B$ is the rate of change of angular momentum relative to body axes; and

$\underline{\omega}$ is the inertial angular velocity.

In body axes,

$$\underline{\omega} = [\omega_s, \omega_2, \omega_3] \qquad [86]$$

and

$$\underline{H} = [I_s\omega_s, I_t\omega_2, I_t\omega_3] \qquad [87]$$

and [85] reads, in components,

$$\omega_s = 0 \qquad [88a]$$

$$\dot{\omega}_2 + \omega_n\omega_3 = 0 \qquad [88b]$$

$$\dot{\omega}_3 - \omega_n\omega_2 = 0 \qquad [88c]$$

where

$$\omega_n = [\frac{I_s}{I_t} - 1]\omega_s \qquad [89]$$

Differentiating [88c] and substituting from [88b] yields

$$\ddot{\omega}_3 + \omega_n^2\omega_3 = 0 \qquad [90]$$

with the solution

$$\omega_3 = A \cos \omega_n t \qquad [91]$$

which, when used in [88b], yields

$$\omega_2 = - A \sin \omega_n t \qquad [92]$$

Let us now suppose that the 2-axis is along the accelerometer axis. Due to the nutation, the test mass experiences a centrifugal acceleration

$$a_c = - \omega_3^2 x = - A^2 x \cos^2 \omega_n t = - \frac{1}{2} A^2(1 + \cos 2\omega_n t)x \qquad [93]$$

If the accelerometer is a simple spring with damping, its equation of motion (neglecting gravity gradients) is then

$$\ddot{x} + 2\lambda\dot{x} + [(K - \omega_s^2 - \frac{1}{2}A^2) - \frac{1}{2}A^2\cos 2\omega_n t]x = \eta g \cos(\omega-\Omega)t \qquad [94]$$

so that, in many respects, the effects of nutation on the system are similar to those of gravity gradients. If the amplitude of the nutation is variable, however, it shifts the resonant frequency of the system, which limits the allowable Q; if the nutation is uncontrolled, we must have, in fact,

$$A < (\omega-\Omega)(2/Q_{eff})^{1/2} \qquad [95]$$

in order to stay within the 3-db bandwidth of the accelerometer, assumed resonant at $(\omega-\Omega)$. For reasonable values of Q_{eff}, this condition can be achieved during start-up of the experiment by the use of nutation damping devices.

The stability of the test masses under nutation may be investigated by the methods of Sec. III.1, using the homogeneous form of [94]. The equation can be reduced to the standard form [35], where now

$$a = (W^2 - \lambda^2)/\omega_n^2 \qquad [96]$$

with

$$W^2 = K - \omega_s^2 - \frac{1}{2}A^2 \qquad [97]$$

and

$$b = (\frac{A}{2\omega_n})^2 \qquad [98]$$

Assuming the damping is small, the system is tuned to the Eötvös signal,

$$a = (\omega-\Omega)^2/\omega_n^2 \qquad [99]$$

and, from [95],

$$b < \frac{1}{2}\left(\frac{\omega-\Omega}{\omega_n}\right)^2/Q_{eff} = \frac{a}{2Q_{eff}} \qquad [100]$$

According to [89], choice of the ratio of moments of inertia allows control of the nutation frequency ω_n which appears in the time-varying coefficient in [94]. As ω_n is varied, according to [100] the operating point in the a-b plane remains closer to the a-axis than a line through the origin, of slope $2Q_{eff}$. For any reasonable Q_{eff}, examination of the stability diagram from the Mathieu equation[25] shows that the solutions of [94] will be stable except for quite restricted regions around

$$a = n^2 \qquad [101]$$

where n is any integer. In other words, the condition [95] is sufficient to ensure stability as long as

$$\omega_n \neq \frac{1}{n}(\omega-\Omega) \qquad [102]$$

or, from [89] (since $\omega_s \simeq \omega$)

$$I_s/I_t \neq 1 + \frac{1}{n}\left(1 - \frac{\Omega}{\omega}\right) \qquad [103]$$

where n is close to integral.

The result [102] merely states that the nutation frequency should not be close to a submultiple of the resonant frequency of the accelerometer. This imposes some constraints on the design of the apparatus: for example, the wheel should not be closely similar to a thin disk in its inertial properties if $\omega >> \Omega$, for then $I_s/I_t = 2$ and approximate equality will hold in [103] for $n = 1$.

b) Gravity-Gradient Torques

The first-order terrestrial gravity gradients exert a torque on the satellite which may be calculated as follows: In an orbital inertial frame (oi-frame), which is an inertially non-rotating frame whose origin is comoving with the CM of the satellite, the net force on an element of mass dm of the satellite, located at vector position r_i with respect to the CM, is (cf.[23])

$$dF_i = \Gamma_{ij} r_j dm = - \Omega^2 [r_i - 3R^{-2} R_i r_i R_j] dm \qquad [104]$$

where it is assumed the satellite is in a circular orbit. In vector notation,

$$d\underline{F} = - \Omega^2 [\underline{r} - 3R^{-2} (\underline{R} . \underline{r}) \underline{R}] dm \qquad [104a]$$

The total torque exerted on the body by the gravity gradient is the integral over the body of the moment of the force [104] (unless otherwise noted, all integrals below are over the body):

$$\underline{M} = \int \underline{r} \times d\underline{F}$$

$$= 3\Omega^2 R^{-2} \int (\underline{R}.\underline{r})(\underline{r} \times \underline{R}) dm$$

$$= -3\Omega^2 R^{-2} \underline{R} \times \underline{J} \qquad [105]$$

where we have used the fact that $\underline{r} \times \underline{r} = 0$ and where

$$\underline{J} = \int (\underline{R}.\underline{r})\underline{r}\, dm \qquad [106]$$

Reverting now to tensor notation, we use the definition [70] of the inertia tensor to write

$$J_i = R_j \int r_j r_i dm = R_j [\int r^2 \delta_{ji} dm - I_{ji}] \qquad [107]$$

The first term on the right, in vector notation, is $\underline{R}\int r^2 dm$, which will vanish when the cross product with $\underline{R}$ is taken in [105]. It is therefore sufficient to consider the vector

$$J_i = -R_j I_{ji} \qquad [108]$$

In principal axes $\underline{i}$, $\underline{j}$, $\underline{k}$ in the body, this vector is

$$\underline{J} = -I_1 \underline{R}.\underline{i}\, \underline{i} - I_2 \underline{R}.\underline{j}\, \underline{j} - I_3 \underline{R}.\underline{k}\, \underline{k} \qquad [109]$$

so that [105] gives

$$\underline{M} = 3\Omega^2 R^{-2} [I_1 (\underline{R}.\underline{i})(\underline{R} \times \underline{i}) + I_2 (\underline{R}.\underline{j})(\underline{R} \times \underline{j}) + I_3 (\underline{R}.\underline{k})(\underline{R} \times \underline{k})] \qquad [110]$$

Assume now that the body has an axis of symmetry, so that

$$I_1 = I_s$$
$$I_2 = I_3 = I_t \qquad [111]$$

and then

$$\underline{M} = 3\Omega^2 R^{-2}[I_s(\underline{R}.\underline{i})(\underline{R} \times \underline{i}) + I_t \underline{R} \times ((\underline{R}.\underline{j})\underline{j} + (\underline{R}.\underline{k})\underline{k})]$$
$$= 3\Omega^2 R^{-2}[I_s(\underline{R}.\underline{i})(\underline{R} \times \underline{i}) + I_t \underline{R} \times (\underline{R} - (\underline{R}.\underline{i})\underline{i})]$$
$$= 3\Omega^2 (I_s - I_t) R^{-2} (\underline{R}.\underline{i})(\underline{R} \times \underline{i}) \qquad [112]$$

The gravity-gradient torque is thus always perpendicular to the plane containing the symmetry axis ($\underline{i}$-axis) and the local vertical, and its magnitude is

$$M = \frac{3}{2}\Omega^2 (I_s - I_t) \sin 2\theta \qquad [113]$$

where θ is the angle between the symmetry axis and the local vertical.

Average torque:

The spin angular momentum is $I_s\omega_s$; comparison with [113] shows that the precessional angular velocity ω_p will be smaller than the orbital angular velocity, approximately in the ratio of Ω to ω_s. In this case, components of the torque at orbital and twice-orbital frequency are largely filtered out by the gyroscopic dynamics. While the effects of these higher-frequency components

should be examined in a more complete analysis, because of the possibility that they might excite resonances which could be mistaken for Eötvös forces, attention is restricted here to the effects of the torque averaged over an orbit.

To compute the average torque, set up a triad of inertially fixed unit vectors $\underline{l},\underline{m},\underline{n}$, with $\underline{n}$ along the orbit normal. Let the components of the symmetry-axis unit vector $\underline{i}$ along these directions be i_1,i_2,i_3: these will be assumed not to change significantly during a single orbit. Measuring the geocentric angle ϕ from the instant when $\underline{l}$ is along the local vertical, we calculate the integral

$$\frac{1}{2\pi}\int_0^{2\pi}(\underline{i}_R\cdot\underline{i})(\underline{i}_R \times \underline{i})d\phi$$

where

$$\underline{i}_R = \underline{l}\cos\phi + \underline{m}\sin\phi \qquad [114]$$

is a unit vector along the local vertical. Now

$$\underline{i}_R\cdot\underline{i} = i_1\cos\phi + i_2\sin\phi \qquad [115]$$

$$\underline{i}_R \times \underline{i} = \begin{vmatrix} \underline{l} & \underline{m} & \underline{n} \\ \cos\phi & \sin\phi & 0 \\ i_1 & i_2 & i_3 \end{vmatrix}$$

$$= i_3\sin\phi\,\underline{l} - i_3\cos\phi\,\underline{m} + (i_2\cos\phi - i_1\sin\phi)\underline{n} \qquad [116]$$

The integral is then

$$\frac{1}{2\pi}\int_0^{2\pi}\{(i_1i_3\sin\phi\cos\phi + i_2i_3\sin^2\phi)\underline{l} - (i_1i_3\cos^2\phi + i_2i_3\sin\phi\cos\phi)\underline{m} + [i_1i_2(\cos^2\phi - \sin^2\phi) + (i_2^2 - i_1^2)\sin\phi\cos\phi]\underline{n}\}\,d\phi \quad [117]$$

which reduces readily to

$$\frac{1}{2}[i_2i_3\underline{l} - i_1i_3\underline{m}] = \frac{1}{2}i_3(\underline{i}\times\underline{n}) = \frac{1}{2}(\underline{i}.\underline{n})(\underline{i}\times\underline{n}) \quad [118]$$

all other terms integrating to zero.

This integral can now be used to find the average value of the torque [112] over an orbit:

$$\overline{\underline{M}} = \frac{3}{2}\Omega^2(I_s - I_t)(\underline{i}.\underline{n})(\underline{i}\times\underline{n}) \quad [119]$$

The average torque is thus perpendicular to $\underline{n}$ (i.e., it lies in the orbital plane) and is of magnitude

$$\overline{M} = \frac{3}{4}\Omega^2(I_s - I_t)\sin 2\gamma \quad [120]$$

where γ is the angle between the symmetry axis and the orbit normal.

c) Gravity-Gradient Induced Precession and Nutation

The relationship between the set of unit vectors $\underline{i},\underline{j},\underline{k}$ along the principal axes of the satellite and the set $\underline{l},\underline{m},\underline{n}$ which are fixed in the oi-frame can be described by three Euler angles, as shown in Fig. V:

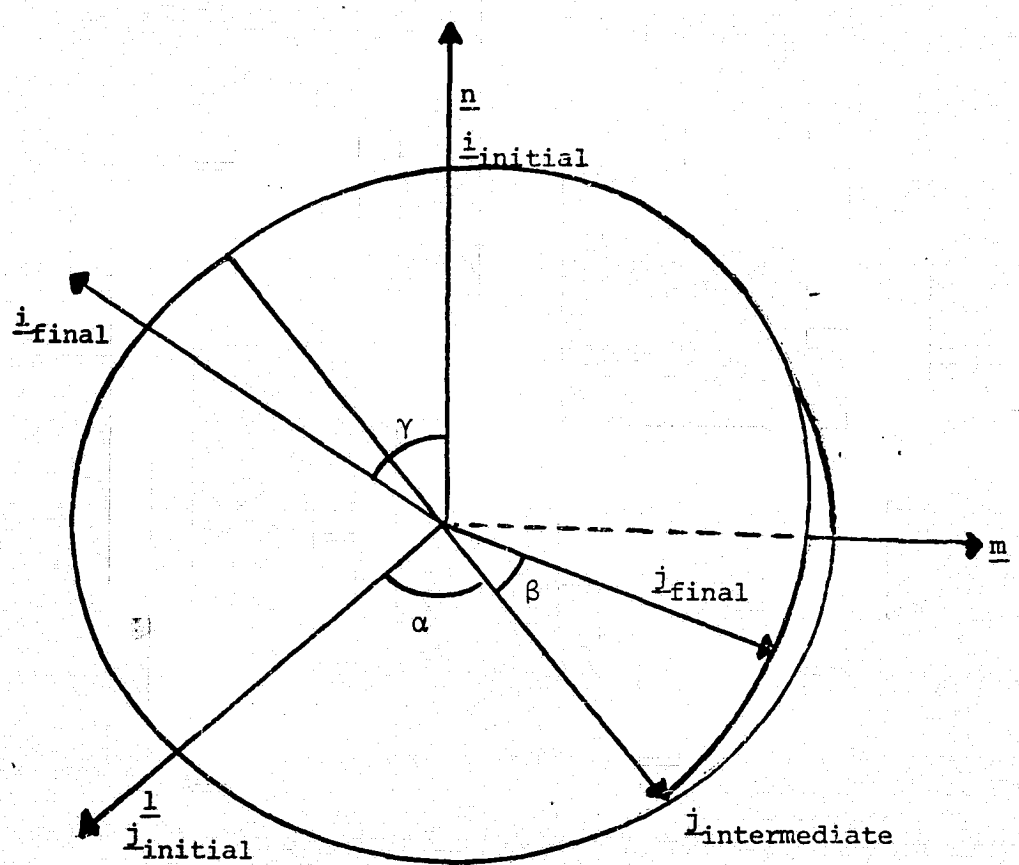

Figure V: Euler Angles for Locating Body Axes Relative to Orbital-Inertial Axes

γ, the angle between the symmetry axis $\underline{i}$ and the orbit normal $\underline{n}$;

α, the azimuth angle of the symmetry axis about $\underline{n}$; and

β, the rotation angle about $\underline{i}$.

The order of rotations from the oi-frame to the body frame (b-frame) is first, a rotation α about $\underline{n}$, a rotation γ about the displaced $\underline{j}$-axis, and finally a rotation β about the displaced $\underline{i}$-axis.

In body axes, the angular velocity of the body is given in terms of the rates of change of the Euler angles by

$$\underline{\omega}^b = \begin{vmatrix} \dot{\beta} + \dot{\alpha}\cos\gamma \\ \dot{\gamma}\sin\beta - \dot{\alpha}\sin\gamma\cos\beta \\ \dot{\gamma}\cos\beta + \dot{\alpha}\sin\gamma\sin\beta \end{vmatrix} = \begin{vmatrix} \omega_1 \\ \omega_2 \\ \omega_3 \end{vmatrix} \qquad [121]$$

and the angular momentum is given by

$$\underline{H}^b = \begin{vmatrix} I_s\omega_1 \\ I_t\omega_2 \\ I_t\omega_3 \end{vmatrix} \qquad [122]$$

There is no component on the average torque [119] along $\underline{i}$ or $\underline{n}$. The components of angular momentum in these directions are therefore conserved. In particular, from [121]*

*a and b are not to be confused with the coefficients in the standard form of the Mathieu equations.

$$I_s\omega_1 = I_s(\dot{\beta} + \dot{\alpha}\cos\gamma) = I_s b = \text{constant} \qquad [123]$$

In body coordinates,

$$\underline{n}^b = \begin{vmatrix} \cos\gamma \\ -\cos\beta\sin\gamma \\ \sin\beta\sin\gamma \end{vmatrix} \qquad [124]$$

so that the component of angular momentum along $\underline{n}$ may be written

$$\underline{H}.\underline{n} = I_s b\cos\gamma + \dot{\alpha} I_t \sin^2\gamma = I_s a = \text{constant} \qquad [125]$$

from [121]. Thus

$$\dot{\alpha} = \frac{\sigma}{\sin^2\gamma}[a - b\cos\gamma] \qquad [126]$$

where

$$\sigma = I_s/I_t \qquad [127]$$

and

$$\dot{\beta} = b - \dot{\alpha}\cos\gamma = b - \frac{\sigma\cos\gamma}{\sin^2\gamma}[a - b\cos\gamma] \qquad [128]$$

We have thus found that $\dot{\alpha}$ and $\dot{\beta}$ depend only on the value of γ. To determine the values of the constants a and b, the variation of γ with time, we need another equation, which can be obtained from the conservation of energy. The rotational kinetic energy is

$$K = \frac{1}{2}[I_s\omega_1^2 + I_t(\omega_2^2 + \omega_3^2)]$$

$$= \frac{1}{2} I_s b + \frac{1}{2} I_t(\dot{\gamma}^2 + \dot{\alpha}^2\sin^2\gamma) \qquad [129]$$

from [121]. The potential energy in the gravity gradient force field may be obtained by integration of the magnitude [120] of the average torque:

$$V = \int_o^\gamma \bar{M}\, d\gamma$$

$$= -\frac{3}{8}\Omega^2(I_s - I_t)\cos 2\gamma \qquad [130]$$

The total energy is then

$$E = K + V = \text{constant} \qquad [131]$$

An equivalent constant of the motion is

$$d = \frac{2}{I_t}[E - \frac{1}{2} I_s b^2] = \dot{\gamma}^2 + \dot{\alpha}^2\sin^2\gamma - \frac{3}{4}\Omega^2(\sigma-1)\cos 2\gamma \qquad [132]$$

since b is constant. Substituting for $\dot{\alpha}$ from [126] yields

$$\dot{\gamma}^2 = -\frac{\sigma^2}{\sin^2\gamma}(a - b\cos\gamma)^2 + \frac{3}{4}\Omega^2(\sigma-1)\cos 2\gamma + d$$

or

$$\sin^2\gamma\,\dot{\gamma}^2 = -\sigma^2(a - b\cos\gamma)^2 + \frac{3}{4}\Omega^2(\sigma-1)\cos 2\gamma\sin^2\gamma + d\sin^2\gamma \quad [133]$$

If we put

$$u = \cos\gamma \quad [134]$$

the equation becomes

$$\dot{u}^2 = f(u)$$

$$= c(1 - u^2)(2u^2 - 1) + d(1 - u^2) - \sigma^2(a - bu)^2 \quad [135]$$

where

$$c = \frac{3}{4}\Omega^2(\sigma-1) \quad [136]$$

The problem has thus been reduced to quadratures, in terms of elliptic integrals. Some useful information may however be derived without carrying through the general integration. For example, the amplitude of the motion in γ may be found by noting that, at the limits of such motion, $\dot{u}$ is zero, and therefore the limits are given by the roots of $f(u)$.

To simplify the discussion, we consider the motion which develops if the spin axis is initially inertially stationary; i.e., we choose the initial conditions $\dot{\alpha} = 0$, $\dot{\gamma} = 0$ at $t = 0$. Let the initial value of u be u_o. Then, from [126] at $t = 0$,

$$a = bu_o \quad [137]$$

and then, since $\dot{u}$ is zero at t = 0, [135] gives

$$d = - c(2u_o^2 - 1) \qquad [138]$$

so that, at general times,[135] may be written

$$\dot{u}^2 = f(u) = 2c(1-u^2)(u^2-u_o^2) - \sigma^2 b^2 (u-u_o)^2$$

$$= (u-u_o)[2c(1-u^2)(u+u_o) - \sigma^2 b^2 (u-u_o)] \qquad [139]$$

Apart from u_o, the roots of f(u) are those of

$$2c(1-u^2)(u+u_o) - \sigma^2 b^2 (u-u_o) = 0 \qquad [140]$$

With the above initial conditions

$$b = \omega_s$$

the spin angular velocity, so that

$$2c/\sigma^2 b^2 = \frac{3}{2}\frac{\Omega^2}{\omega_s^2}(\sigma-1)/\sigma^2 << 1 \qquad [141]$$

if the spin angular velocity is much greater than the orbital angular velocity. An approximate solution to the cubic [140] may be found by writing it in the form

$$u - u_o = \frac{2c}{\sigma^2 b^2}(1 - u^2)(u + u_o) \qquad [142]$$

According to [141], the quantity on the right is small, so that the root is close to u_o, which means in turn that u may be replaced by u_o on the right, to give the approximate root

$$u_1 = u_o[1 + \frac{4c}{\sigma^2 b^2}(1 - u_o^2)] \qquad [143]$$

The other two roots of [140] are imaginary.

If now we write

$$u_o = \cos \gamma_o$$
$$u_1 = \cos(\gamma_o + \delta_1) \simeq \cos \gamma_o - \delta_1 \sin \gamma_o \qquad [144]$$

and insert these into [143], we obtain

$$\delta_1 = -\frac{3}{2}\frac{(\sigma-1)}{\sigma^2}(\Omega/\omega_s)^2 \sin 2\gamma_o \qquad [145]$$

for the amplitude of the gravity-gradient induced nutation (i.e., fluctuation in γ). The effect is very small indeed, less than 0.1 seconds of arc if $\omega_s \simeq 10$ rpm, in low orbit.

The nutation frequency may be obtained by writing

$$u = \cos(\gamma_o + \delta) = \cos \gamma_o - \delta \sin \gamma_o \qquad [146]$$

When this is inserted in [139], we obtain, to second order in δ,

$$\dot{\delta}^2 = -\delta[A_1 + A_2\delta] \qquad [147]$$

where

$$A_1 = 2c \sin 2\gamma_o \qquad [148]$$

$$A_2 = \sigma^2 b^2 + 2c(5u_o^2 - 1) \simeq \sigma^2 b^2 \qquad [149]$$

The solution of [147], meeting the initial conditions, is

$$\delta = \frac{1}{2}\delta_1(1 - \cos \omega_n t) \qquad [150]$$

where

$$\omega_n = \sigma \omega_s \qquad [151]$$

is the nutational frequency. Comparison with [89] shows that the induced nutation has the same frequency as the free-body nutation. Since its amplitude is so small, it is expected to have a negligible effect compared with the free-body effect.

The precessional angular velocity can now be obtained from [126]:

$$\dot{\alpha} = \frac{\sigma b}{\sin^2\gamma}(u_o - u) \simeq \frac{\sigma b \delta}{\sin \gamma_o}$$

$$= \frac{1}{2}\sigma\omega_s\delta_1 \frac{(1 - \cos \omega_n t)}{\sin \gamma_o} \qquad [152]$$

The precession thus varies with time, ranging from zero to twice the average value

$$\omega_p = \frac{1}{2}\sigma\omega_s\delta_1/\sin \gamma_o$$

$$= \frac{3}{2}\frac{\Omega^2}{\omega_s}\left(\frac{\sigma-1}{\sigma}\right)\cos \gamma_o \qquad [153]$$

As seen from the oi-frame, the motion thus consists of a steady coning of the spin axis around the orbit normal at the angular

velocity (153], with a very small superimposed circular motion, with an amplitude $\frac{1}{2}\delta_1$.

In order to find the effects on the experiment of precessional motion, we neglect the nutation. Then [128] gives

$$\dot{\beta} = \omega_s \qquad [154]$$

If the accelerometer sensitive axis is along the 2-axis, the test mass experiences a centrifugal acceleration given by

$$a_c = -\omega_3^2 x = \omega_p^2 x \sin^2\gamma_o \sin^2\omega_s t \qquad [155]$$

from [121].

This is similar to the form [93] found for free-body nutation, except that A is replaced by $\omega_p \sin \gamma_o$ and ω_n by ω_s. One may then carry through a similar investigation of the stability of the solutions of the resulting Mathieu equation of motion. Analogously to [99] and [98], the coefficients in the standard form of the Mathieu equation are found to be in this case

$$a = (1 - \frac{\Omega}{\omega_s})^2 \qquad [156]$$

and

$$b = [\frac{\omega_p \sin \gamma_o}{2\omega_s}]^2 = [\frac{3}{8}(\frac{\sigma-1}{\sigma}) \sin 2\gamma_o]^2 (\Omega/\omega_s)^4 \qquad [157]$$

By elimination of (Ω/ω_s), one can obtain an equation showing the path followed by the operating point in the a-b plane as this parameter is varied. It is not difficult to see that this path is confined to the stable region near the origin in Fig. IV.

It thus appears that gravity-gradient induced nutation and precession should not have a significant effect on operation of the experiment. The effects can, of course, be minimized by making γ_o as small as possible, but stringent tolerances in the alignment of the spin axis with the orbit normal do not appear to be required.

A more detailed analysis nevertheless should be carried out, retaining higher frequency terms in the gravitational torque [112], which were eliminated in the averaging process to obtain [119].

III.3 Conclusions from Systems Analysis

We have now considered in some detail the first four of the possible disturbances listed in Sec. III.2. No effects have been found which might prevent operation of the experiment down to the design sensitivity of one part in 10^{14} in the measurement of the Eötvös ratio.

It appears to be possible to carry out a useful experiment in the payload bay of the shuttle, if it is feasible to locate the experiment reasonably close to the CM of the shuttle and if the RCS system can be used to fly the shuttle so as to follow the experiment. An average fuel flow of order 5 kg/hour would probably be sufficient for this task.

The STS (shuttle) provides an ideal vehicle for carrying out this experiment, which can make good use of the capabilities of the crewmen. If flown unmanned, the very sensitive accelerometers

would require caging to withstand the boost environment and some form of orbital gyrocompassing would be needed in order to erect the wheel spin axis to the orbit normal. Furthermore, if it is desired to measure the Eötvös ratio of several materials, a mechanism would be required for changing the test masses. Finally, experience with the low-level accelerometers in orbit[32] suggests that difficulties may arise which are very difficult to solve in an automatic system. The crewman may make final design choices as the result of on-orbit experience (e.g., in selecting servo compensation networks), deploy the system in its optimum configuration, monitor the performance and investigate any anomalies observed, and modify the experiment (e.g., by installing new test masses) to extend the investigation. At the same time, the equipment may be considerably simpler than would be needed for an unmanned launch.

The development program for this experiment might involve three separate shuttle-born phases. In the first, component parts of the apparatus (particularly the accelerometer) would be tested in free fall, so that commitment to final development could be postponed until the design performance had been demonstrated. In the second phase, a limited experiment would be carried out in the payload bay, if further analysis shows that this is feasible and that significant simplifications could be effected by operation in this mode. Finally, (and particularly if any Eötvös anomalies were discovered in the second phase), a fully autonomous experiment would be launched from the shuttle, at the maximum sensitivity which may prove feasible.

CHAPTER FOUR

DESIGN OF A MAGNETIC MICROBALANCE FOR ACCELEROMETER TEST

IV.1 Introduction

As discussed in Chapter II, the heart of the orbital Eotvos experiment is a very sensitive dual accelerometer, the two test masses being constructed from the materials whose ratio of gravitational to inert mass is being compared. In low orbit and in the absence of external disturbances, the sensitivity of this accelerometer, in gees, is equal to the limiting accuracy in measurement of the Eötvös ratio. For example, to reach an accuracy of $\eta = 10^{-15}$ in the experiment, the dual accelerometer must be capable of detecting a relative acceleration between the test masses of 10^{-15}g. This is many orders of magnitude beyond the sensitivity of conventional accelerometers, so that design of the accelerometer system becomes the most critical task in development of the experiment. The frequency at which the acceleration must be measured can however be chosen by fixing the angular velocity of the apparatus, a freedom which can be used to discriminate against some sources of measurement noise.

At the present time, both cryomagnetic and electrostatic techniques for suspension of the test masses are under study, the first primarily at Stanford and the second at M.I.T.

A fundamental difficulty in the development of any sensitive accelerometer for use in space is that, if the device is to be tested on Earth, much stronger suspension forces than are needed in orbit must be provided. This problem has, in the past, generally led either to design compromises or to a reliance on analytical design techniques, without specific test of the final configuration before commitment to flight.

In the Bell Miniature Electrostatic Accelerometer (MESA), for example, the gap between the test mass and the supporting electrode structure is comparable to that normally found in electrostatically supported instruments for terrestrial application (i.e., thousandths of an inch), so that it can be operated on Earth by applying not unreasonably high voltages. For operation in space, the electrode voltage is merely reduced, so as to provide support against the expected small transverse accelerations. The cross-coupling between forces along the suspension axes and the sensitive axis, which is due primarily to geometrical imperfections of the test mass and electrodes, electrode edge effects, etc., is thus no better than in terrestrial instruments, and little advantage is taken of the benign orbital environment to maximize performance.

Most satellites designed for "pure gravity orbit" are examples of the other approach to this problem. Such satellites are driven so as to follow an unsupported test mass, which is protected from external forces.[32] This system can be regarded as an accelerometer which is sensitive to accelerations in all three axes. It is essential to minimize the forces (primarily electrostatic and gravitational) which are applied to the test mass by the satellite itself. This is usually achieved by careful analytical design, but there is generally little opportunity to test the resulting concept except by an actual flight in space.

An interesting approach to testing an electrostatically-supported space instrument is that of de Bra et al[33], in which a test mass of sufficiently low density is used so that it may be floated in a heavy gas (SF_6). This technique is not however considered applicable to the problem of testing accelerometer designs for the Eötvös experiment: it obviously will not work at the low temperatures required in a cryomagnetic suspension and, at the higher temperatures which may be used with an electrostatic suspension, it introduces convective disturbances and damping forces.

In order to allow experimental investigation of design concepts for an electrostatically-supported accelerometer for the orbital Eötvös experiment, it would be highly desirable to simulate free fall in the laboratory. The feasibility of using magnetic forces for this purpose is investigated in this chapter.

Magnetic suspensions have of course been employed for a wide variety of purposes. The present concept is unusual in that it is desired, not to provide stable suspension of the test mass, but to buck out its weight, using forces generated by appropriate suspension coils, in such a way that additional magnetic forces do not result when the test mass is displaced from its nominal position. With the magnetic suspension providing the main support force and neutral stability, an electrode structure can be built to control the test mass whose dimensions and voltages are similar to those which might be used in space.

It is assumed here initially that the magnetic material embedded in the test mass is linear -- i.e., the magnetization vector induced in it is proportional to the external field. The reasons for this condition and means for implementing it are discussed in Section IV.5 below.

IV.2 Basic Relationships

The force on a sample of linear magnetic material in an external field $\underline{B}$ is given by[34]

$$\underline{F} = k \nabla B^2 \qquad [158]$$

where k is a constant depending on the size, shape and magnetic properties of the object. If the body is diamagnetic (e.g., if it is superconducting), k is negative.

The external field is given in terms of the vector potential $\underline{A}$ by

$$\underline{B} = \nabla \times \underline{A} \qquad [159]$$

and the vector potential is given by an integral over the current density $\underline{J}$ in the coils:

$$\underline{A} = \frac{\mu^\circ}{4\pi} \int \frac{\underline{J}(\underline{r}')}{|\underline{r} - \underline{r}'|} d^3r' \qquad [160]$$

where μ° is the permeability of free space and $\underline{r}$, $\underline{r}'$ are vectors from the origin of coordinates to the observation point and to a source point in the coils, respectively.

For constructional simplicity, it is proposed to build the suspension from a set of cylindrical coils of rectangular cross-section, with the symmetry axis (the z-axis) vertical. Figure VI shows a vertical section through one of the coils: the centroid of the cross-section is at radius b and height a above the origin, and the cross-sectional area measures 2β by 2α. The current density has only a circumferential component, which is

$$J_\phi = nI \qquad b-\beta < r' < b+\beta \quad a-\alpha < z' < a+\beta$$
$$= 0 \qquad \text{elsewhere} \qquad [161]$$

where I is the current and n the number of turns/unit area.

Because of the cylindrical symmetry, we may choose the observation point in the r-z plane. From the geometry of the perspective sketch of the coil shown in Figure VII, we may write

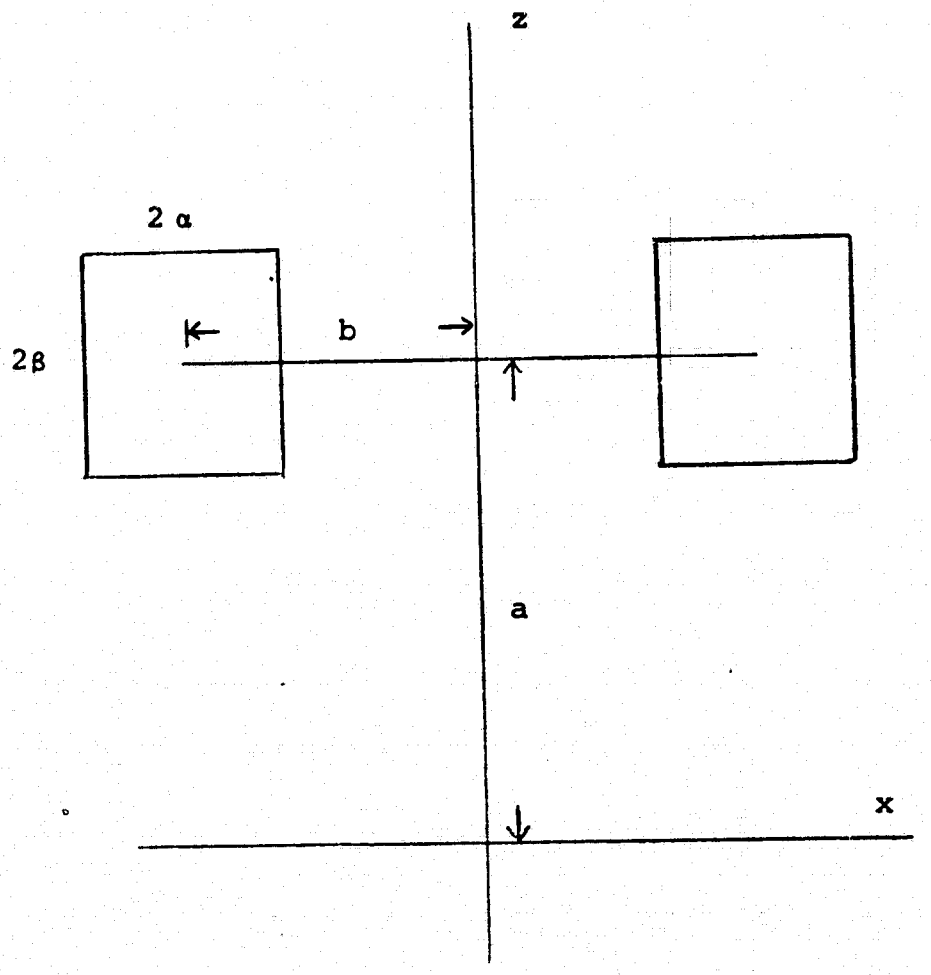

Figure VI. Coil Cross-Section

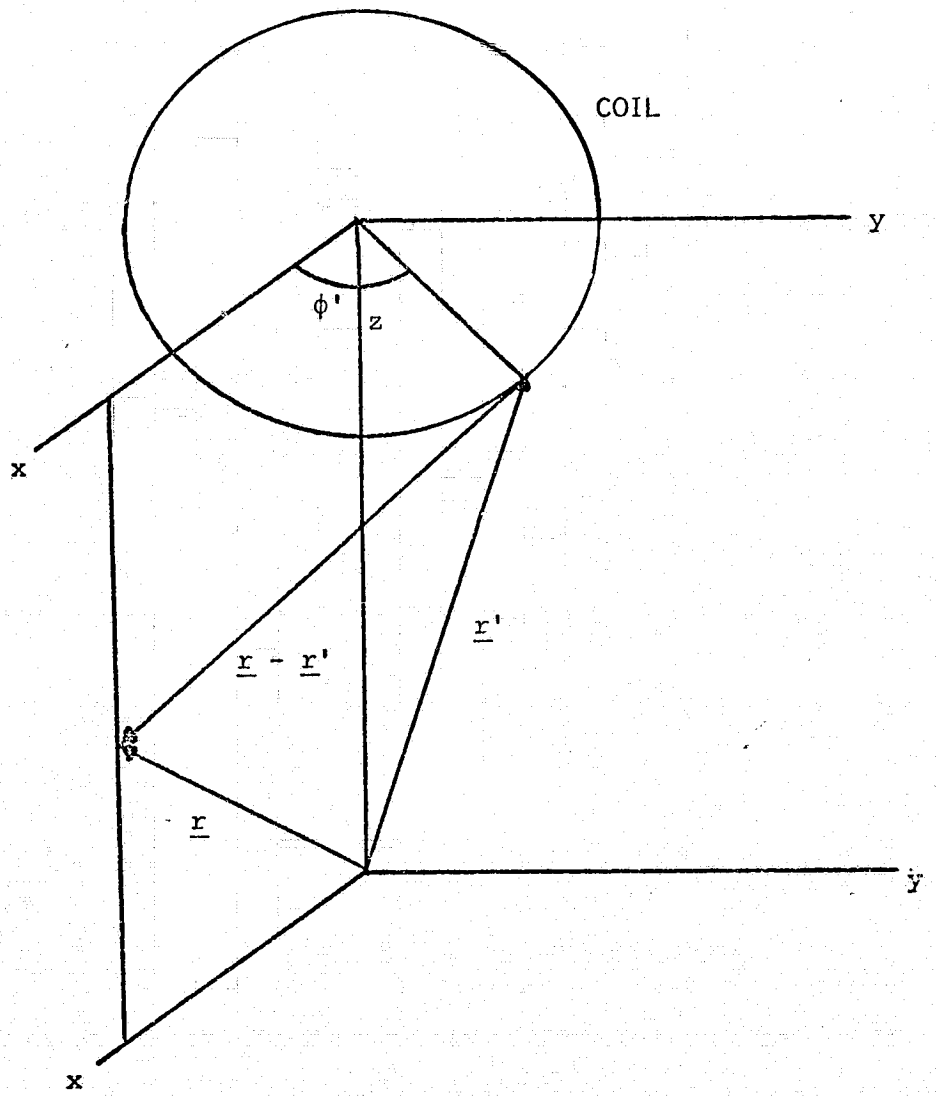

Figure VII: Geometry of Source and Observation Points

$$f(r,z) = |\underline{r} - \underline{r}'|^{-1}$$

$$= [(z-z')^2 + r^2 + r'^2 - 2rr'\cos\phi']^{-1/2} \qquad [162]$$

where ϕ' is the angle between the horizontal projections of $\underline{r}$ and $\underline{r}'$.

To compute the integral [160], we must write $\underline{J}$ in rectangular components, which are

$$J_x = -J_\phi \sin\phi'$$
$$[163]$$
$$J_y = J_\phi \cos\phi'$$

It is clear from [160] that $\underline{A}$ also has only a circumferential component, so that, at the observation point, the integral over J_x must vanish. The vector potential from all the coils can then be written

$$A_\phi = \frac{\mu^\circ}{4\pi} \sum_{\text{coils}} nI \int_{b-\beta}^{b+\beta} r'dr' \int_{a-\alpha}^{a+\alpha} dz' \int_0^{2\pi} f(r,z)\cos\phi'\, d\phi' \qquad [164]$$

The ϕ'-integral may be expressed in elliptic integrals, but, for present purposes, it is more convenient to expand $f(r,z)$ in a Taylor series in r about the symmetry axis, so that the integral becomes

$$\Phi = \int_0^{2\pi} [f^\circ + rf^{i}(0,z) + \frac{1}{2}r^2 f^{ii}(0,z) + \frac{1}{3!}r^3 f^{iii}(0,z)$$
$$+ \frac{1}{4!}r^4 f^{iv}(0,z) + \frac{1}{5!}r^5 f^{v}(0,z) + \ldots]\cos\phi'\, d\phi' \qquad [165]$$

where $f^n(0,z) = \left.\frac{\partial^n F}{\partial r^n}\right|_{r=0}$, so that

$$f^\circ = f(0,z) = [(z-z')^2 + r'^2]^{-1/2} \qquad [166]$$

A straightforward computation of the indicated derivatives of [162] with respect to r yields

$$f^{i}(0,z) = f^{\circ 3} r' \cos\phi' \qquad [167a]$$

$$f^{ii}(0,z) = 3f^{\circ 5} r'^2 \cos^2\phi' - f^{\circ 3} \qquad [167b]$$

$$f^{iii}(0,z) = 3[5f^{\circ 7} r'^3 \cos^3\phi' - 3f^{\circ 5} r' \cos\phi'] \qquad [167c]$$

$$f^{iv}(0,z) = 3[35f^{\circ 9} r'^4 \cos^4\phi' - 30f^{\circ 7} r'^2 \cos^2\phi' + 3f^{\circ 5}] \qquad [167d]$$

$$f^{v}(0,z) = 15[63f^{\circ 11} r'^5 \cos^5\phi' - 70f^{\circ 9} r'^3 \cos^3\phi' + 15f^{\circ 7} r' \cos\phi'] \qquad [167e]$$

When these expressions are used in [165], all odd powers of $\cos\phi'$ integrate to zero. We are left with

$$\Phi = \pi[f^{\circ 3} r' r + \frac{3}{2}(\frac{5}{4} f^{\circ 7} r'^3 - f^{\circ 5} r') r^3 + \frac{15}{8}(\frac{21}{8} f^{\circ 11} r'^5 - \frac{7}{2} f^{\circ 9} r'^3 + f^{\circ 7} r') r^5 + \ldots] \qquad [168]$$

The vector potential may thus be written

$$A_\phi = Q(z) r + K(z) r^3 + N(z) r^5 + \ldots \qquad [169]$$

where

$$Q(z) = \frac{\mu^\circ}{4} \sum_{\text{coils}} nI \int_{b-\beta}^{b+\beta} \int_{a-\alpha}^{a+\alpha} r'^2 f^{\circ 3} dr' dz' \qquad [170]$$

$$K(z) = \frac{3}{8}\mu^{\circ} \sum_{\text{coils}} nI \int_{b-\beta}^{b+\beta} \int_{a-\alpha}^{a+\alpha} [\frac{5}{4} f^{\circ 7} r'^{4} - f^{\circ 5} r'^{2}] dr'dz' \qquad [171]$$

$$N(z) = \frac{15}{32}\mu^{\circ} \sum_{\text{coils}} nI \int_{b-\beta}^{b+\beta} \int_{a-\alpha}^{a+\alpha} [\frac{21}{8} f^{\circ 11} r'^{6} - \frac{7}{2} f^{\circ 9} r'^{4} + f^{\circ 7} r'^{2}] dr'dz' \qquad [172]$$

If we differentiate [170] under the integral twice with respect to z (denoted by primes), we obtain the important result

$$Q''(z) = -8K(z) \qquad [173]$$

From [159], in cylindrical coordinates, the axial and radial components of the magnetic field are given by

$$B_z = \frac{1}{r}\frac{\partial}{\partial r}(rA_{\phi})$$

$$= 2Q(z) + 4K(z)r^2 + 6N(z)r^4 + \ldots \qquad [174]$$

and

$$B_r = -\frac{\partial}{\partial z} A_{\phi}$$

$$= -[Q'(z)r + K'(z)r^3 + N'(z)r^5 + \ldots] \qquad [175]$$

Using [173], the square of the magnetic field is then

$$B^2 = B_z^2 + B_r^2$$

$$= 4Q^2(z) + (Q'^2(z) + 16K(z)Q(z))r^2$$

$$+ 2(8K^2(z) + Q'(z)K'(z) + 12Q(z)N(z))r^4 + O(r^6)$$

$$= 4Q^2(z) + (Q'^2(z) - 2Q(z)Q''(z))r^2$$

$$+ 2(8K^2(z) + Q'(z)K'(z) + 12Q(z)N(z))r^4 + O(r^6) \qquad [176]$$

Since there is no term linear in r, there is, at the origin of coordinates, only an axial component of force (as one would expect from symmetry), which is, from [158],*

$$F_z = 8kQ^\circ Q^{\circ\prime} \qquad [177]$$

where $Q^\circ = Q(0)$, $Q^{\circ\prime} = \frac{d}{dz}Q(z)\Big|_{z=o}$

The objective of the suspension is to simulate free fall: the support force should be as nearly constant as possible (and equal to the weight of the suspended object) in a region around the origin. In Cartesian tensor notation, the force at a position x_i ($i = 1,2,3$, with the 3-axis vertical) is given by a Taylor expansion around the origin

$$F_i = F_i^\circ + S_{ij}x_j + \Gamma_{ijk}x_j x_k + \ldots \qquad [178]$$

where

$$F_i^\circ = k\frac{\partial}{\partial x_i}B^2\Big|_{x_i=o} \qquad [179]$$

$$S_{ij} = k\frac{\partial^2}{\partial x_i \partial x_j}B^2\Big|_{x_i,x_j=0} \qquad [180]$$

$$\Gamma_{ijk} = \frac{k}{2}\frac{\partial^3}{\partial x_i \partial x_j \partial x_k}B^2\Big|_{x_i,x_j,x_k=0} \qquad [181]$$

The simulation will be successful at the origin if we can make the stiffnesses S_{ij} zero, and the "playing area" (i.e., the region

*Notice that, to give an upward force, Q° and $Q^{\circ\prime}$ must be of opposite sign if $k < 0$ and of the same sign if $k > 0$.

in which the simulation is acceptable) will be maximized if we can also make the second-order stiffnesses Γ_{ijk} zero. In calculating these quantities, we take derivatives of [176] and then place $r = 0$, so it is clear that we can neglect the term in r^4. In the present notation, [176] thus becomes

$$B^2 = 4Q^2 + (Q'^2 - 2QQ'')(x_1^2 + x_2^2) + \ldots \qquad [182]$$

where Q is a function of x_3 alone.

The force is now

$$F_i = k\begin{vmatrix} 2(Q'^2 - 2QQ'')x_1 \\ 2(Q'^2 - 2QQ'')x_2 \\ 8QQ' - 2QQ'''(x_1^2 + x_2^2) \end{vmatrix} \qquad [183]$$

which, at the origin, of course reduces to [177].

The matrix of second derivatives of B^2 is

$$\frac{\partial^2 B^2}{\partial x_i \partial x_j} = \begin{vmatrix} 2(Q'^2-2QQ'') & 0 & -4QQ''' x_1 \\ 0 & 2(Q'^2-2QQ'') & -4QQ''' x_2 \\ -4QQ''' x_1 & -4QQ''' x_2 & 8(Q'^2+QQ'')-2(Q'Q''' +QQ''')(x_1^2+x_2^2) \end{vmatrix} \qquad [184]$$

At the origin, the only surviving components are the radial stiffness

$$S_r = S_{11} = S_{22} = 2k(Q^{\circ\prime 2} - 2Q^{\circ}Q^{\circ\prime\prime}) \qquad [185]$$

and the vertical stiffness

$$S_z = S_{33} = 8k(Q^{\circ\prime 2} + Q^\circ Q^{\circ\prime\prime}) \qquad [186]$$

It is clear from these expressions that S_z and S_r cannot both be zero. Moreover, in conformity with Earnshaw's theorem, it is impossible to make the suspension stable in all directions if k is positive. We therefore choose to make the radial stiffness zero, relegating control along the vertical axis to an external stabilization system (see below). The design goal is thus

$$Q^{\circ\prime 2} = 2Q^\circ Q^{\circ\prime\prime} \qquad [187]$$

Note that, when this condition holds, the vertical stiffness becomes

$$S_z = 12kQ^{\circ\prime 2} \qquad [188]$$

so that the system is vertically stable for diamagnetic test masses ($k < 0$) and unstable for $k > 0$. A useful figure of merit for suspensions of this type is the characteristic length

$$Z = F_z/S_z = \frac{2}{3}\frac{Q^\circ}{Q^{\circ\prime}} \qquad [189]$$

which will be negative if $k < 0$ and positive if $k > 0$.

For a given support force, Z is maximized (i.e., the vertical inhomogeneity is minimized) by making Q° as large as possible and $Q^{\circ\prime}$ small. Under the condition [187],

$$Q^{\circ\prime\prime} = \frac{1}{2}Q^{\circ\prime 2}/Q^\circ = \frac{1}{3}Q^{\circ\prime}/Z \qquad [190]$$

and so must be small but finite.

The second-order stiffnesses, calculated by taking the derivatives of [184], form a three-dimensional matrix, but most of the terms vanish at the origin. By inspection, we find in fact that the finite terms are

$$\Gamma_{113} = \Gamma_{131} = \Gamma_{223} = \Gamma_{232} = \Gamma_{311} = \Gamma_{322} = -2k\varrho^\circ\varrho^{\circ\prime\prime\prime}$$
$$\Gamma_{333} = 4k(3\varrho^{\circ\prime}\varrho^{\circ\prime\prime} + \varrho^\circ\varrho^{\circ\prime\prime\prime}) \qquad [191]$$

The expansion [178] of the force may now be written in vector form as

$$\underline{F} = k[8\varrho^\circ\varrho^{\circ\prime} + 8(\varrho^{\circ\prime 2}+\varrho^\circ\varrho^{\circ\prime\prime})z - 2\varrho^\circ\varrho^{\circ\prime\prime\prime}(x^2+y^2) + 4(3\varrho^{\circ\prime}\varrho^{\circ\prime\prime}+\varrho^\circ\varrho^{\circ\prime\prime\prime})z^2]\underline{i}_z$$
$$+ k[2(\varrho^{\circ\prime 2}-2\varrho^\circ\varrho^{\circ\prime\prime})x - 4\varrho^\circ\varrho^{\circ\prime\prime\prime}xy)\underline{i}_x$$
$$+ k[2(\varrho^{\circ\prime 2}-2\varrho^\circ\varrho^{\circ\prime\prime})y - 4\varrho^\circ\varrho^{\circ\prime\prime\prime}xy)\underline{i}_y \qquad [192]$$

where $\underline{i}_x, \underline{i}_y, \underline{i}_z$ are unit vectors along the axes.

If the condition [187] holds and if, in addition, we can achieve

$$\varrho^{\circ\prime\prime\prime} = 0 \qquad [193]$$

then the force reduces to

$$\underline{F} = k[8\varrho^\circ\varrho^{\circ\prime} + 12\varrho^{\circ\prime 2}z + 12\varrho^{\circ\prime}\varrho^{\circ\prime\prime}z^2]\underline{i}_z \qquad [194]$$

or

$$\underline{F} = \underline{F}^{\circ}[1 + \frac{z}{Z} + \frac{1}{3}(\frac{z}{Z})^2] \qquad [195]$$

Achievement of these conditions thus means that, to the second order in the displacement of the suspended object from the origin, no forces are generated in the horizontal plane. Furthermore, the variation in the vertical force is independent of horizontal displacements, to this order. The quadratic term in [195] merely means that the vertical stabilization servo should have a slightly non-linear characteristic.

The quantities needed for design of this system are obtained from [170] as

$$Q^{\circ} = \frac{1}{4}\mu^{\circ} \sum_{\text{coils}} nI \int_{b-\beta}^{b+\beta} \int_{a-\alpha}^{a+\alpha} r'^2(z'^2+r'^2)^{-3/2} dr'dz' \qquad [196]$$

$$Q^{\circ\prime} = -\frac{3}{4}\mu^{\circ} \sum_{\text{coils}} nI \int_{b-\beta}^{b+\beta} \int_{a-\alpha}^{a+\alpha} r'^2 z'(z'^2+r'^2)^{-5/2} dr'dz' \qquad [197]$$

$$Q^{\circ\prime\prime} = \frac{3}{4}\mu^{\circ} \sum_{\text{coils}} nI \int_{b-\beta}^{b+\beta} \int_{a-\alpha}^{a+\alpha} r'^2(4z'^2-r'^2)(z'^2+r'^2)^{-7/2} dr'dz' \qquad [198]$$

$$Q^{\circ\prime\prime\prime} = -\frac{15}{4}\mu^{\circ} \sum_{\text{coils}} nI \int_{b-\beta}^{b+\beta} \int_{a-\alpha}^{a+\alpha} r'^2 z'(4z'^2-3r'^2)(z'^2+r'^2)^{-9/2} dr'dz' \qquad [199]$$

IV.3 Ideal Coil Design

To simplify selection of a configuration for the suspension, we assume at first that the coils are of infinitesimal cross-section. The above expressions then take on the simple forms

$$Q^\circ = \frac{1}{4}\mu^\circ \sum_{\text{coils}} NI\, b^2 (a^2+b^2)^{-3/2} \qquad [196a]$$

$$Q^{\circ\prime} = \frac{3}{4}\mu^\circ \sum_{\text{coils}} NI\, b^2 a (a^2+b^2)^{-5/2} \qquad [197a]$$

$$Q^{\circ\prime\prime} = \frac{3}{4}\mu^\circ \sum_{\text{coils}} NI\, b^2 (4a^2-b^2)(a^2+b^2)^{-7/2} \qquad [198a]$$

$$Q^{\circ\prime\prime\prime} = \frac{15}{4}\mu^\circ \sum_{\text{coils}} NI\, b^2 a (4a^2-3b^2)(a^2+b^2)^{-9/2} \qquad [199a]$$

where N is the number of turns in each coil. To reiterate, the conditions we wish to achieve are [187] and [193]:

$$Q^{\circ\prime 2} = 2Q^\circ Q^{\circ\prime\prime} \qquad [200]$$

and

$$Q^{\circ\prime\prime\prime} = 0 \qquad [201]$$

At the same time, we wish to maximize the support force at the origin

$$F_z^\circ = 8kQ^\circ Q^{\circ\prime} \qquad [202]$$

and the length which characterizes the vertical homogeneity

$$z = \frac{2}{3}Q^\circ/Q^{\circ\prime} \qquad [203]$$

IV.3.1 Single-Coil Suspension

Let us first consider the possibility of a suspension using a single coil. From the above expressions, the condition [200] gives, for this case

$$a^2 = \frac{2}{5}b^2 \qquad [204]$$

There is thus a point on the axis of a thin coil of radius b, at a distance $\sqrt{\frac{2}{5}}\,b$ from the plane of the coil, where the transverse gradients of the magnetic force vanish. At this point, the characteristic length (203) is

$$z = \frac{2}{a}\,\frac{a^2+b^2}{a} = \frac{7}{9}\sqrt{\frac{2}{5}}\,b \approx .492\,b \qquad [205]$$

The support force is

$$F^\circ = 8kQ^\circ Q^{\circ\prime}$$

$$= \frac{3}{2}\,\frac{b^4 a}{(a^2+b^2)^4}\,k\mu^{\circ 2}N^2I^2$$

$$= \frac{3}{\sqrt{10}}\left(\frac{5}{7}\right)^4\,\frac{k\mu^{\circ 2}N^2I^2}{b^3}$$

$$\approx 0.247\,\frac{k\mu^{\circ 2}N^2I^2}{b^3} \qquad [206]$$

It is clearly impossible to satisfy the condition [201] at this point. We therefore turn to suspensions containing two or more coils.

IV.3.2 Helmholtz Coils

From [198a], Q°'' vanishes is

$$a = \frac{1}{2}b \qquad [207]$$

or if the coil lies on a cone with apex at the origin and semivertex angle

$$\phi_H = \tan^{-1}2 = 63.43^\circ \qquad [208]$$

Now suppose we have a pair of such coils, symmetrically located at $Z = \pm a$ on the Helmholtz cone, with the same number of turns in each and the same current flowing. Then [196a] to [199a] give for the pair

$$Q^\circ = \frac{1}{2}\mu^\circ NIb^2(a^2+b^2)^{-3/2}$$

$$= \frac{2}{5^{3/2}}\frac{\mu^\circ NI}{a} \qquad [208a]$$

$$Q^{\circ\prime} = Q^{\circ\prime\prime} = Q^{\circ\prime\prime\prime} = 0 \qquad [208b]$$

This is, of course, the Helmholtz coil arrangement which is frequently used to produce a uniform magnetic field.

If the current in the Helmholtz pair flows in opposite senses, we obtain

$$Q^\circ = Q^{\circ\prime\prime} = 0 \qquad [210a]$$

$$Q^{\circ\prime} = \frac{3}{2}\mu^\circ NI\, b^2a(a^2+b^2)^{-5/2}$$

$$= \frac{6}{5^{5/2}}\frac{\mu^\circ NI}{a^2} \qquad [210b]$$

$$Q^{\circ'''} = \frac{15}{2}\mu^{\circ}NI\ b^2a(4a^2-3b^2)(a^2+b^2)^{-9/2}$$

$$= -\frac{48}{5^{7/2}}\frac{\mu^{\circ}NI}{a^4} \qquad [210c]$$

Neither a Helmholtz nor anti-Helmholtz pair, by itself, can provide a lift force.

IV.3.3 Maxwell Coils

From [199a], $Q^{\circ'''}$ vanishes if

$$a^2 = \frac{3}{4}b^2 \qquad [211]$$

or if the coil lies on a cone with apex at the origin and semi-vertex angle

$$\phi_M = \tan^{-1}\frac{2}{\sqrt{3}} = 49.11^{\circ} \qquad [212]$$

A pair of similar coils, symmetrically located at $Z = \pm a$ on the Maxwell cone, with current in the same sense, yield

$$Q^{\circ} = \frac{1}{2}\mu^{\circ}NI\ b^2/(a^2+b^2)^{3/2} = \frac{2\sqrt{3}}{7^{3/2}}\frac{\mu^{\circ}NI}{a} \qquad [213a]$$

$$Q^{\circ''} = \frac{3}{2}\mu^{\circ}NI\ b^2(4a^2-b^2)/(a^2+b^2)^{7/2} = \frac{16.3^{5/2}}{7^{7/2}}\frac{\mu^{\circ}NI}{a^3} \qquad [213b]$$

$$Q^{\circ'} = Q^{\circ'''} = 0 \qquad [213c]$$

If the currents are in opposite senses, we obtain

$$Q^{\circ} = Q^{\circ''} = Q^{\circ'''} = 0 \qquad [214a]$$

$$Q^{\circ\prime} = \frac{3}{2}\mu^{\circ}NI\ b^2a/(a^2+b^2)^{5/2} = 2\left(\frac{3}{7}\right)^{5/2}\frac{\mu^{\circ}NI}{a^2} \qquad [214b]$$

IV.3.4 Coil Combinations

It should be clear that, by appropriate choice of Helmholtz and Maxwell coils, it is possible to provide independent control of Q°, $Q^{\circ\prime}$, $Q^{\circ\prime\prime}$, $Q^{\circ\prime\prime\prime}$, as follows:

1) Q° alone is generated by a Helmholtz pair.

2) $Q^{\circ\prime}$ alone is generated by an anti-Maxwell pair.

3) $Q^{\circ\prime\prime}$ alone may be generated by a Maxwell pair, together with a Helmholtz pair so connected as to subtract the Q° generated by the Maxwell pair.

4) $Q^{\circ\prime\prime\prime}$ will be zero, as desired, if the suspension is made up of combinations of the above coil sets.

Suppose we wish to generate $Q^{\circ\prime\prime}$ alone. For a compact design, it will be convenient to use a Maxwell pair and a Helmholtz pair with the same radius b. For stability, we assume the same current I is flowing in both sets of coils (i.e., they are wired in series). From [213b] and [211] the Maxwell pair, with N_M turns in each coil, produces

$$Q^{\circ\prime\prime} = \frac{384}{7^{7/2}}\frac{\mu^{\circ}N_MI}{b^3} \qquad [215]$$

but it also produces an unwanted

$$Q^{\circ} = \frac{4}{7^{3/2}}\frac{\mu^{\circ}N_MI}{b} \qquad [216]$$

This can be compensated by a Helmholtz pair of N_H turns each, with current flowing in the opposite sense, to give

$$Q^\circ = - \frac{4}{5^{3/2}} \frac{\mu^\circ N_H I}{b} \qquad [217]$$

from [209a]. We thus require

$$N_M/N_H = \left(\frac{7}{5}\right)^{3/2} = 1.657 \simeq \frac{53}{32} \qquad [218]$$

IV.3.5 A Maxwell-Coil Suspension

The Maxwell coil has the advantage that $Q^{\circ\prime\prime\prime} = 0$ automatically. If we now consider a pair of coils, symmetrically located on the Maxwell cone, with the same current I flowing but with N_1 turns in the upper coil and N_2 in the lower, [196a] to [199a] give

$$Q^\circ = \frac{1}{4} \mu^\circ I \, (N_1+N_2) b^2/(a^2+b^2)^{3/2}$$
$$= \frac{2}{7^{3/2}} (N_1+N_2) \frac{\mu^\circ I}{b} \qquad [219]$$

$$Q^{\circ\prime} = \frac{3}{4} \mu^\circ I (N_1-N_2) b^2 a/(a^2+b^2)^{5/2}$$
$$= \frac{12\sqrt{3}}{7^{5/2}} (N_1-N_2) \frac{\mu^\circ I}{b^2} \qquad [220]$$

$$Q^{\circ\prime\prime} = \frac{3}{4} \mu^\circ I (N_1+N_2) b^2 (4a^2-b^2)/(a^2+b^2)^{7/2}$$
$$= \frac{192}{7^{7/2}} (N_1+N_2) \frac{\mu^\circ I}{b^3} \qquad [221]$$

$$Q^{\circ\prime\prime\prime} = 0 \qquad [222]$$

The condition [200] is now

$$9(N_1-N_2)^2 = 8(N_1+N_2)^2 \qquad [223]$$

The solutions of this equation are easily seen to be

$$N_1/N_2 = \frac{3+\sqrt{8}}{3-\sqrt{8}} = 34 \qquad [224]$$

or the inverse of this. Which coil is to have more turns is readily determined by considering the force at the origin, which is

$$F^\circ = 8kQ^\circ Q^{\circ\prime}$$

$$= \frac{192\sqrt{3}}{7^4}(N_1^2 - N_2^2)\, k\, \frac{\mu^{\circ 2} I^2}{b^3} \qquad [225]$$

The lower coil must have the greatest number of turns in the test mass is diagmagnetic ($k < 0$). Test masses of equal but opposite susceptibility could be supported by merely inverting the suspension.

With [224], the support force becomes

$$F^\circ = 0.138\,|k|\,\mu^{\circ 2} N^2 I^2/b^3 \qquad [226]$$

where N is now the number of turns in the larger coil.

Comparison with [206] shows that, for coils of the same radius and number of turns and the same current, the single coil suspension produces a considerably stronger force than this Maxwell suspension. However, the characteristic length for the Maxwell suspension is, from [219] and [220]

$$Z = \frac{14}{12\sqrt{3}}\,\frac{N_1+N_2}{N_1-N_2}\,b = .714b \qquad [227]$$

which is considerably better than the single-coil case. In other words, the vertical inhomogeneity is less pronounced.

As it stands, this suspension nominally meets the design requirements. However, in order to allow for construction tolerances, it is proposed to add an extra set of Helmholtz and Maxwell coils, outside the main coils, connected as discussed in the previous Section so as to produce Q°" only. Current flowing in these trim coils should have no effect on the lift force nor on the characteristic length, but can be used to trim the radial stiffness of the suspension to zero.

The resulting coil configuration is shown in Fig. VIII. Some modifications to the turns ratios are required when the finite cross-sections of the coils are taken into account (i.e., when [196] to [199] are used instead of [196a] to [199a]).

IV.3.6 Vertical Servo

Varying the current in the coils will not affect the conditions [200] and [201], but it will change the vertical force. This effect can be used to compensate for the gradients in the vertical force indicated by [195], using the measured vertical displacement of the proof mass to control the current. This feedback control is essential for stability if the proof mass is not diamagnetic.

To simplify current stabilization it is proposed to provide an additional pair of coils (called the servo coils), having turns n_1 and n_2 in the ratio [224] and situated on the Maxwell cone.

C-2

For simplicity, it is assumed here that the servo coils are wound with the main coils, although they might have to be separated if the inductive coupling between the two sets of coils is excessive (especially if superconducting coils are used). An accurately stabilized current I then flows in the main coils, while a current i(z) flows in the servo coils, in response to the measured vertical displacement z of the proof mass. The vertical equation of motion is now

$$m\ddot{z} = k'(NI + ni(z))^2 \left[1 + \frac{z}{Z} + \frac{1}{3}\left(\frac{z}{Z}\right)^2 + \ldots\right] - mg \qquad [228]$$

where, from [226],

$$k' = 0.138\,|k|\,\frac{\mu^{\circ 2}}{b^3} \qquad [229]$$

and N, n are the numbers of turns in the larger of the main and servo coils, respectively. Since it is assumed that the larger coil is the lower (upper) one, according as the proof mass is diamagnetic (paramagnetic), k' is always a positive quantity. Recall, however, that Z is negative for diamagnetic proof masses.

If the main coil current is adjusted so as to balance the weight of the proof mass at the origin, then from [226]

$$mg = k'(NI)^2 \qquad [230]$$

and [228] becomes

$$\ddot{z}/g = \left[2\left(\frac{ni(z)}{NI}\right) + \left(\frac{ni(z)}{NI}\right)^2\right]\left(1 + \frac{z}{Z} + \frac{1}{3}\left(\frac{z}{Z}\right)^2 + \ldots\right)$$

$$+ \frac{z}{Z} + \frac{1}{3}\left(\frac{z}{Z}\right)^2 + \ldots \qquad [231]$$

We now write

$$i(z) = \frac{NI}{n}\left(C_1\frac{z}{Z} + C_2\left(\frac{z}{Z}\right)^2\right) \qquad [232]$$

in [231]. Retaining only up to quadratic terms gives

$$\ddot{z}/g = (2C_1 + 1)\frac{z}{Z} + (2C_1 + C_1^2 + 2C_2 + \frac{1}{3})(\frac{z}{Z})^2 + \ldots \simeq C \qquad [233]$$

if

$$C_1 = -\frac{1}{2}$$

$$C_2 = \frac{5}{24} \qquad [234]$$

If, then, we make

$$i(z) = \frac{1}{2}\frac{N_1 I}{n_1}(-\frac{z}{Z} + \frac{5}{12}(\frac{z}{Z})^2 + \ldots) \qquad [235]$$

this servo control will make the first- and second-order vertical force gradients zero at the origin.

Under these conditions, the suspension will support the magnetic proof mass in a neutrally stable region near the origin: no additional forces are produced, up to the second order in displacements in any direction from the origin.

The objective of this suspension is to buck out the weight of a test mass so that it may be mounted in a weak electrostatic suspension of the type which might be used in the Eötvös experiment in free fall. In testing such an accelerometer, it is expected that the sensitive axis will be horizontal. The displacement detector required for the electrostatic support in this accelerometer may provide the signal for the vertical magnetic servo.

It is clear that this system provides a high degree of isolation to the proof mass from vibrations of the support structure

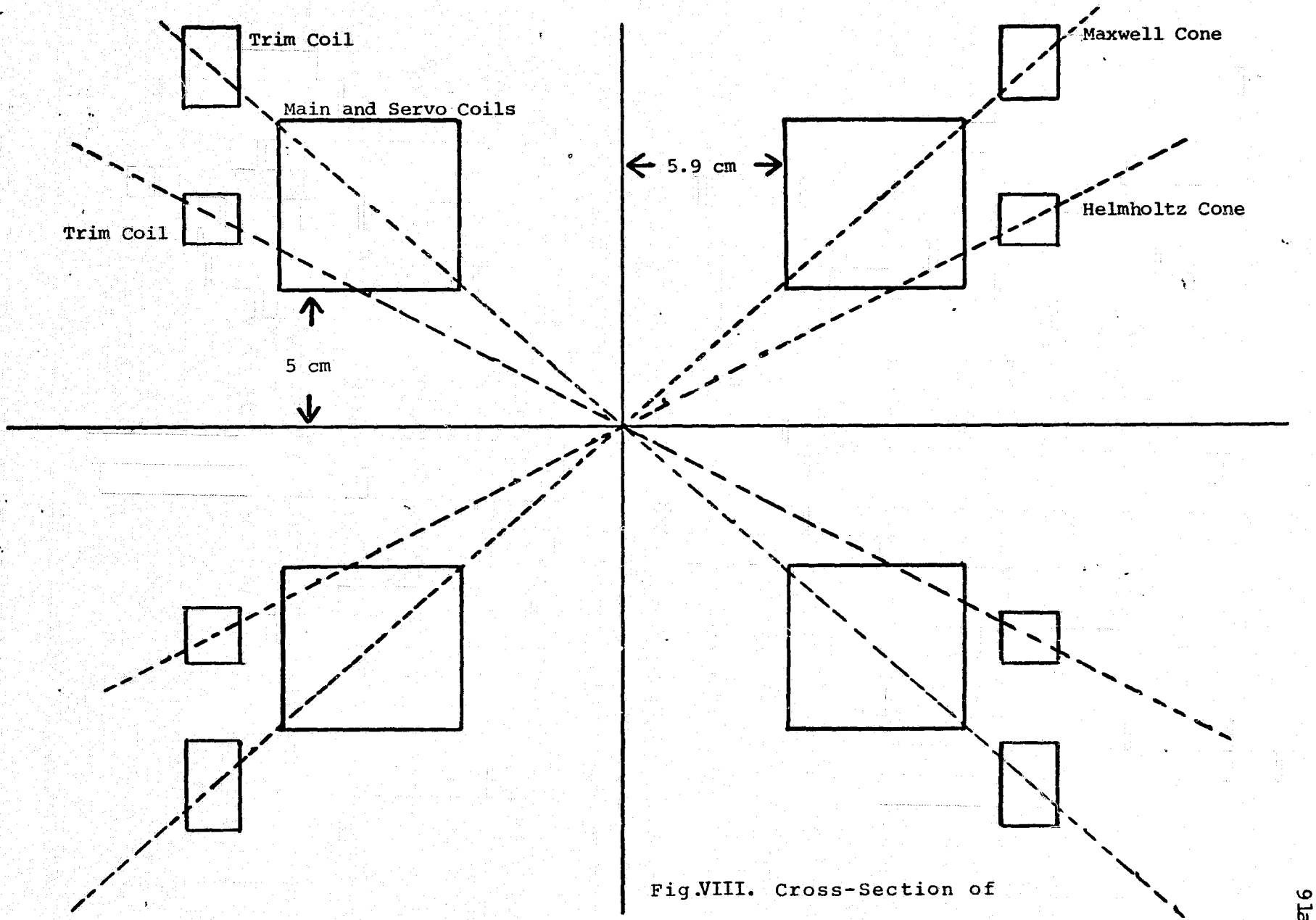

Fig.VIII. Cross-Section of Magnetic Suspension

(e.g., microseisms), since the suspension force is invariant up to the second order in displacements relative to the coils. The system is however sensitive to relative vibrations of the component parts. For example, suppose that the displacement detector for the vertical magnetic servo is displaced vertically by a distance ε, relative to the coils, while the proof mass is at the origin (z=0). The signal to the vertical servo will then be $-\varepsilon$ and the current in the servo coil will be, by [235]

$$i = \frac{1}{2}\frac{N_1 I \varepsilon}{n_1 Z} \qquad [236]$$

to the first order. According to [228], the force produced on the test mass will be approximately

$$F = k'(N_1 I)^2 \varepsilon/Z$$

$$= mg\varepsilon/Z \qquad [237]$$

from [230]. The system must therefore be sufficiently rigid so that relative vibrations of its component parts, in the frequency range of interest, are very small compared to the characteristic length Z.

IV.4 Disturbing Magnetic Fields

The vertical component of any external, spatially uniform, constant magnetic field merely adds a constant term, presumably small, to Q(z) in [174]. This will make a small change in the vertical force at the origin, according to [177], and it will also change slightly the radial stiffnesses, an effect which may be compensated by current in the trim coils so as to maintain the condition [187].

The horizontal component of any external field is somewhat more troublesome. Suppose that there is an external field B_e along the x_1-axis, so that the magnetic field within the suspension is

$$\underline{B} = \begin{vmatrix} B_r \sin \phi + B_e \\ B_r \cos \phi \\ B_z \end{vmatrix} \qquad [238]$$

where ϕ is an azimuth angle and B_r, B_z are given by [175], [174], respectively. The square of the field is then

$$B^2 = B_z^2 + B_r^2 + B_e^2 + 2B_e B_r \sin \phi$$

$$= B_o^2 + B_e^2 - 2B_e \left[Q'(x_3)x_1 + K'(x_3)(x_1^2 + x_2^2)x_1 + \ldots\right] \qquad [239]$$

from [175]. B_o is the field in the absence of the external field.

The force on the proof mass when it is at the origin is given by [179]. The first-order effect of the external field is thus to produce an additional force in the x_1-direction given by

$$F_1 = -2kB_e Q''$$

$$= -\frac{1}{2}\frac{B_e}{B_o} mg \qquad [240]$$

from [177] and [174].

It appears from this equation that the field of the Earth, in particular, will produce an acceleration of the proof mass in the north-south direction whose magnitude, depending on the value achieved for B_o, may be of order one milligee. In using the suspension for accelerometer test, it would of course be possible to

orient the sensitive axis east-west (or, more generally, perpendicular to the horizontal component of any external field). If it is desired to simulate free fall to higher accuracy, it would be necessary to buck out the external field, for example by a large Helmholtz coil pair, outside the suspension with its axis horizontal. The maximum field produced by this compensating coil need only be of order 0.2 gauss, and its direction and magnitude could be adjusted so as to produce a null field at the origin with the suspension switched off, as measured by a magnetometer.

It is important to avoid time-varying external magnetic fields, especially in the frequency range of interest for testing accelerometers. In principle, it would be possible to measure the variable component of the external magnetic field with a 3-axis magnetometer situated outside the suspension (and far enough away so that it is not swamped by the main suspension field). The signal produced could be used to vary the main (or servo) coil current, the trim coil current, and external Helmholtz compensation coil currents in such a way as to null the forces on the proof mass, but it is highly desirable to avoid this additional complexity.

From [240], the 60 Hz field due to power wiring will produce a jitter in the position of the proof mass, but the amplitude will be only a few hundred Angstroms even if the field amplitude reaches one gauss. This effect is therefore negligible.

In the calculations presented here, it has been assumed that the suspension is constructed of ideal coils, of infinitesimal

cross-section. It is not difficult to show that the requisite suspension conditions [187] and [193] can be achieved using coils of finite cross-section. Realistic calculations require other design decisions about the suspension (in particular, whether it is to be constructed of superconducting coils or not) and therefore are not reproduced here.

Disturbing magnetic fields can be produced by two other mechanisms: (i) errors and distortions in winding the coils, so that the turns density is not uniform and the shape is not identical to that assumed in the calculation; and (ii) distortions of the suspension field due to magnetic materials in its vicinity. To some extent these disturbances, being constant, may be corrected using the trim and compensation coils, but it is clearly desirable, from [240], to keep the fractional distortion of the field as small as possible. The limits to the simulation of free fall imposed by manufacturing tolerances have not yet been thoroughly studied. It is, in any case, important to build the support structure for the suspension from non-magnetic materials.

IV.5 Proof Mass Design

In the work presented here it has been assumed that the magnetic material of the proof mass is linear -- i.e., that its magnetic moment may be written[34]

$$\underline{M} = \chi_m V \underline{H} \qquad [241]$$

where V is the volume of magnetic material and χ_m is its magnetic susceptibility. Under these circumstances, the change in energy in the suspension when the proof mass is introduced, with the coil currents held constant, is

$$U = \frac{1}{2}\,\underline{M}.\underline{B}_o \qquad [242]$$

where $B_o = \mu_o \underline{H}$ is the field without the proof mass. The force exerted by the magnetic field is then

$$\underline{F} = \nabla U = \frac{1}{2}\nabla(\underline{M}.\underline{B}_o) = \frac{1}{2}\frac{\chi_m}{\mu_o}\nabla\nabla B_o^2 \qquad [243]$$

from [241]. This is of the form [158].

In order to achieve strong support forces, the obvious choice is to use a ferromagnetic proof mass. In this case, however, [242] is only a rough approximation, especially when hysteretic effects are included: the energy may depend on the path by which the proof mass is introduced to the suspension. Furthermore, the force on a ferromagnetic proof mass will not generally be of the form [243], even if [242] may be taken as sufficiently accurate. The use of magnetically soft and hard materials must be considered separately.

IV.5.1 Magnetically Soft Proof Mass

If the magnetic field is sufficiently weak, a soft ferromagnetic object will exhibit a linear relationship similar to [241] (neglecting hysteresis). A reasonable support force can then be provided by using a strong gradient in the magnetic field at the origin. Unfortunately, a weak field and a strong gradient leads, according to [189], to a small value of the characteristic length Z of the suspension.

In order to build a suspension of adequate performance, it is almost certainly necessary to use a field at the origin which is strong enough so that the proof mass is saturated. The magnitude of the magnetic moment will then be fixed, but its direction will

be along the external field, or nearly so. We may thus write

$$\underline{M} = M_o \, \underline{i}_B \qquad [244]$$

where M_o is the saturated magnetic moment and $\underline{i}_B$ is a unit vector along the original field. Then [243] gives

$$\underline{F} = \frac{1}{2} M_o \, \nabla B \qquad [245]$$

so that the force is proportional to the gradient of the magnitude of the field, rather than to the gradient of the square of the field. The analysis given in this chapter then fails. It may still be possible to build a suspension with the desired properties using a soft magnetic proof mass, but the analysis will be considerably more complicated.

IV.5.2 Magnetically Hard Proof Mass (Permanent Magnet)

If the proof mass contains a permanent magnet whose magnetic moment is $\underline{M}_o$ and whose dimensions are much smaller than the characteristic length Z in the field, it will experience a torque given by

$$\underline{T} = \underline{M}_0 \times \underline{B} \qquad [246]$$

In the absence of restraining forces, the magnetic moment will execute an oscillation about the field direction at an angular frequency given by

$$\omega^2 = M_o B / m\xi^2 \qquad [247]$$

where m is the mass and ξ the radius of gyration about an axis perpendicular to the magnetic axis of the proof mass. Assuming for the moment that the period of this oscillation is very much less than the time constants characteristic of rectilinear

motion of the proof mass in the suspension, and that there is some damping of the angular oscillation (e.g., by eddy currents), the magnetic moment may be taken as being along the field direction in calculating the force on the proof mass. Equation [244] then applies and, at the origin, the force is given by [245] as

$$\underline{F} = - m\underline{g} = \frac{1}{2} M_o \nabla B \qquad [248]$$

According to [174], the field and field gradient at the origin are given by

$$B_z = 2Q^\circ$$

$$\partial B_z/\partial z = 2Q^{\circ\prime} \qquad [249]$$

so that [247] and [248] give

$$\omega^2 = \frac{2g}{\xi^2} \frac{B}{\nabla B} = \frac{2g}{\xi^2} \frac{Q^\circ}{Q^{\circ\prime}} = \frac{3gZ}{\xi^2} \qquad [250]$$

The angular frequency of oscillation is then that of a pendulum of length $\xi^2/3Z$ and will generally be quite high if the magnet is small, as assumed in this section.

An important difference between the hard and soft cases is that, if the magnetic moment is aligned with the field, a permanent magnet must physically rotate when it is displaced horizontally from the origin. It is easily seen from [174] and [175] that the magnetic field at a radial distance r from the origin makes an angle

$$\theta \simeq - \frac{r}{3Z} \qquad [251]$$

A proof mass containing such a magnet must therefore exhibit a rocking motion when it oscillates horizontally, an undesirable defect in the simulation of free fall.

A possible solution to this difficulty arises from the observation that, unlike the soft case, it is not necessary to provide a magnetic field at the origin when a permanent magnet is used. Apart from second-order effects unaccounted for in [246], the torque vanishes at the origin if the field is zero there -- i.e., by [174] and [175], if $Q^\circ = 0$. In the use of the suspension for accelerometer test, the magnetic moment may then be kept vertical by relatively small torques exerted by the electrostatic suspension system. We then have

$$\underline{M} = M_o \, \underline{i}_z \qquad [252]$$

where $\underline{i}_z$ is a unit vector along the vertical. Equation [242] then becomes

$$U = \frac{1}{2} M_o B_z = M_o \left[Q(z) - \frac{1}{4} Q''(z)(x^2+y^2) + \ldots \right] \qquad [253]$$

from [174] and [175]. The force at the origin is then given by

$$\underline{F} = \nabla U \big|_{x,y,z=0} = M_o \, Q^{\circ\prime} \, \underline{i}_z = Q^{\circ\prime} \underline{M} \qquad [254]$$

and the stiffnesses at the origin are

$$S_{ij} = M_o \begin{vmatrix} -\frac{1}{2} Q^{\circ\prime\prime} & 0 & 0 \\ 0 & -\frac{1}{2} Q^{\circ\prime\prime} & 0 \\ 0 & 0 & Q^{\circ\prime\prime} \end{vmatrix} \qquad [255]$$

The only non-vanishing terms in the 3-dimensional second-order stiffness matrix are

$$\Gamma_{113} = \Gamma_{131} = \Gamma_{223} = \Gamma_{232} = \Gamma_{322} = \Gamma_{311} = -\frac{1}{2} Q^{\circ\prime\prime\prime}$$
$$\Gamma_{333} = Q^{\circ\prime\prime\prime} \qquad [256]$$

It thus appears that a suspension using a permanent magnet can be constructed by choosing a suspension coil configuration such that

$$Q^\circ = Q^{\circ\prime\prime} = Q^{\circ\prime\prime\prime} = 0 \qquad [257]$$

with $Q^{\circ\prime}$ finite. It was shown in Sec. IV.3.4 that an anti-Maxwell pair (i.e., a pair of identical coils, symmetrically located on the Maxwell cone, with the same current flowing in opposite directions through them) meets these specifications.

Notice that, in this permanent-magnet suspension, it appears to be possible to make the first- and second-order force gradients all zero. By Earnshaw's theorem, it would clearly be necessary to provide some form of feedback stabilization, but the lowest order terms in the destabilizing force appear to be cubic in the displacement from the origin. The performance of the system may thus be superior to that using a linear magnetic proof mass: in particular, it may be less sensitive to the type of relative vibrations of the components discussed in Sec. IV.3.6.

This interesting possibility deserves further investigation. For a permanent magnet, the principal defect of [242] is that it assumes that the proof mass is a perfect magnetic dipole. In a more complete analysis, multipole moments would be expected to interact with higher-order gradients of the magnetic field. As it turns out, however, the desired configuration is one in which at least the next two gradients of the field vanish, according to [257], so that the dipole approximation may prove quite accurate.

IV.5.3 Diamagnetic Proof Mass

We now return to the question of constructing a proof mass of magnetically linear material, for use in a suspension of the type described in previous sections.

With the impractical exception of liquid oxygen,[34] the diamagnetic or paramagnetic susceptibilities of ordinary simple magnetic materials are too small to allow their use in a suspension employing reasonable (kilogauss) fields and field gradients. As is well known, however, a superconducting body is perfectly diamagnetic - i.e., its permeability is zero.

One solution to the problem, which may be practical if the suspension coils are superconducting (so as to maximize the achievable field and eliminate problems with heat dissipation), is to embed a superconducting element inside the proof mass, which will otherwise be constructed of nonmagnetic materials. To eliminate torques on the proof mass, the superconducting element may be spherical. Its magnetic moment is then given in Gaussian units by[35]

$$\underline{M} = -\frac{3}{8\pi}\,\underline{V}\,\underline{B} \qquad [258]$$

where V is its volume. The force is then given in cgs units by

$$\underline{F} = -\frac{3}{16\pi}\,V\,\nabla B^2 \qquad [259]$$

so that, in [158]

$$k = -\frac{3}{16\pi}\,V \qquad [260]$$

The principal difficulties expected in the use of a superconducting proof mass are those that have been encountered in the

development of superconducting gyroscopes. These are:

(i) Elimination of trapped flux. In order that the suspended superconducting sphere not exhibit a permanent magnetic moment and hence anomalous forces, great care must be taken during the transition to the superconducting state. To avoid trapping the field of the Earth, it may be necessary to provide a mechanism whereby the proof mass may be kept outside the suspension, in the normal state, while the suspension coils are cooled and supercurrents established. The proof mass would then be inserted part way into the suspension, to a region where there is a definite field gradient in all directions, and allowed to cool until transition occurs. Only then would it be moved to the center of the suspension.

(ii) Cooling of the suspended proof mass. If the proof mass is suspended in vacuum, it can be cooled only by radiation, a very inefficient process at cryogenic temperatures. The total power dissipation in the proof mass (for example, due to eddy currents in the non-superconducting parts) must be of the order of nanowatts. This condition may be relaxed by retaining a pressure of several torr of helium around the proof mass, so as to provide a convective mechanism for heat dissipation.

An alternative possibility, avoiding the problems of a superconducting proof mass, is to use a pseudo-diamagnetic test body of the type which has been investigated by Wilk[36]. In this concept, the magnetic element in the proof mass would consist of

three concentric, orthogonal coils of small cross-section, with a 3-axis (Hall effect) magnetometer at their center. The three coils carry currents delivered by servo amplifiers so as to drive the magnetic field at the center to zero. The element then behaves very nearly like a perfectly diamagnetic body.

An active proof mass of this type of course requires a power source for the coils and internal electronics. However, in Wilk's analysis, the power requirements were found to be only of order 15 mW per gram of lift force, so that the possibility exists of building a proof mass with an internal power dissipation below one watt. If so, the power could be supplied by a photovoltaic cell forming one end of the proof mass, illuminated by a light beam with a power of order 5 watts.

At the present time, neither the superconducting nor pseudo-diamagnetic proof masses have been adequately studied. The latter type, in particular, requires careful analysis in order to optimize the internal coil design for this application.

CHAPTER FIVE

CONCLUSIONS AND RECOMMENDATIONS

V.1 The Magnetic Microbalance

The analysis presented in Chapter IV has shown interesting possibilities for simulation of free fall in the testing of accelerometers. Of particular promise are magnetic suspensions using either (i) a linear magnetic element consisting of a Wilk pseudo-diamagnet[39]; or (ii) a permanent magnet with its axis vertical, embedded in the proof mass. The suspension coil design to eliminate first- and second-order force gradients at the origin is quite different in these two cases and further work is required before a choice can be made between them.

The original motivation for this study of magnetic suspensions was that it is impossible to test in the laboratory electrostatic accelerometers of the sensitivity required for the orbital Eötvös experiment, if it is necessary to buck out the weight of the proof mass with electrostatic forces. For the specific purposes of the Eötvös experiment, it may now be more cost-effective

to test candidate accelerometer designs on an early flight of the shuttle (STS), rather than to construct a suspension of the type considered here. It is estimated that a shuttle accelerometer test facility could be constructed as a "minilab"[37] weighing less than 200 kg. The direct launch cost, according to the NASA pricing formula[38] and not including allowance for the services of a payload specialist, may be less than $200,000.

To allow resolution of this issue, it is recommended that studies of the magnetic microbalance be continued to the point where a choice can be made between the above two types, the desirability of using superconducting coils in the suspension can be evaluated, and a realistic cost estimate for an operating system can be prepared. A parallel study should be undertaken of an accelerometer test facility for flight in the STS, so that shuttle interfaces may be identified, crew involvement specified, and preliminary estimates made of RDT&E expenses. Comparison of the cost and expected performance of the terrestrial and orbital accelerometer test options will provide the data needed for the orbital Eötvös experiment development plan.

In making this decision, it should be noted that there are applications of the magnetic microbalance other than development of the Eötvös experiment. These include:

(1) Use of the apparatus as a facility for testing electrostatic accelerometer designs for other space applications, in guidance and control of low-thrust vehicles, control of the attitude dynamics of satellites, establishment of "pure gravity orbit"

satellites, etc. Once the system has been built, its use for these purposes will be much cheaper and more convenient than tests carried out on STS missions.

(2) Construction of a sensitive long-period seismometer/tiltmeter based on the microbalance.

(3) Use of two microbalances to support the proof masses in an electromagnetically coupled gravitational-wave antenna[39] for use on Earth. The isolation from microseismic and other disturbances provided by the system is particularly important for this application. Experience gained with such a terrestrial instrument, especially if it proved possible to detect gravitational radiation from one of the expected cosmic sources (e.g., the Crab pulsar) would be of great value in the design of a larger and more sensitive antenna for deployment in orbit by the STS.

V.2 The Orbital Eötvös Experiment

As discussed in Section III.3, the present state of development of the experiment allows confidence that it will prove possible to compare the ratios of passive to inert mass of various materials in orbit with a sensitivity of at least one part in 10^{14}. This will allow a preliminary evaluation of the passive mass of energy stored in the weak interaction. Further analysis is however required to ensure that none of the possible disturbances listed in Section III.2 (or others) will preclude operation at the design sensitivity.

The following immediate tasks have been identified for further development of the experiment:

(1) Continued analysis of disturbing forces.

(2) Establishment of a firm candidate design for a dual electrostatic accelerometer for this application. Of particular importance is a realistic servo design to allow evaluation of the discrimination which is feasible against the identified disturbances.

(3) Development of a plan for testing the accelerometer design, either using the magnetic microbalance or as an experiment on an early STS flight, as discussed above.

(4) More detailed analysis of the feasibility of an Eötvös experiment to be carried out in the payload bay of the shuttle, including identification of shuttle performance limitations, shuttle and crew interfaces, etc. If the performance suggested by preliminary analysis is confirmed, finalization of system design for this experiment.

(5) Firm estimates of the performance improvement which may be achieved by use of an autonomous, free-flying experiment which is erected in and launched from the shuttle. If the expected performance warrants, detailed system design for this experiment.

(6) Development of a firm program plan, including cost and schedule estimates, for carrying out the various phases of the Eötvös experiment which are discussed above.

REFERENCES

1. Bondi, H.: Revs. Modern Phys., 29, 3 (1957), p. 423.
2. Dicke, R.H.: "The Theoretical Significance of Experimental Relativity," Gordon & Breach, N.Y. 1964, p. 77.
3. Schiff, L.I.: Proc. Nat. Acad. Sci., 45, (1959), 69.
4. Lightman, A.P. & Lee, D.L.: Phys. Rev. D, 8, 2(1974)p.364ff.
5. Eotvos, R.von, Pekar, D., & Feteke, E.: Ann. Physik 68,11(1922).
6. Roll, P.G., Krotkov, R., & Dicke, R.H.: Annals of Physics 26, 442 (1964).
7. Braginsky, V.B., & Panov, V.I.: Sov. Phys. - JETP 34, 464ff(1971).
8. Misner, C.W., Thorne, K.S., & Wheeler, J.A.: "Gravitation," Freeman, San Francisco, 1971, p. 1067.
9. Thirring, W.E.: Annals of Physics, 16, 96ff (1961).
10. Chapman, P.K., M.I.T. Experimental Astronomy Lab. Report TE-16 (1966).
11. Chapman, P.K., in preparation.
12. Segre, E.: Nuclei and Particles, Benjamin, N.Y. 1965, p. 215.
13. Schiff, L.I.: Proc. Nat. Acad. Sci., 45, (1959), 69.
14. Blin-Stoyle, R.J.: Phys. Rev. 118, 1605 (1960).
15. Nordvedt, K.: Icarus 12, 91 (1970).
16. Shapiro, I.I., et al: Phys Rev. Letters 36, #11(1976) p.555. Williams, J.G. et al: Phys Rev. Letters 36, #11(1976) p. 551.
17. Misner, C.W., Thorne, K.S. & Wheeler, J.A.: "Gravitation," Freeman, San Francisco, 1971, p. 1061.
18. Sciama, D.W.: Nuova Cim. 8, 417 (1958).
19. Schiff, L.I.: ITP-291, Stanford University (1968) unpublished.
20. Jackson, J.D.: Classical Electrodynamics, Wiley, N.Y.(1962), p. 469.

21. Chapman, P.K.: ASME Paper 70-Av/SpT-16, 1970.

22. Chapman, P.K. & Hanson, A.J.: Proc. Conf. on Experimental Tests of Gravitational Theories, Caltech, Nov. 1970.

23. Worden, P.W.Jr.:A Cryogenic Test of the Equivalence Principle, Thesis, Stanford University, 1976.

24. DeBra, D.B.: Proc. Conf. on Experimental Tests of Gravitational Theories, Caltech, Nov. 1970.

25. McLachlan, N.W.: Theory and Application of Mathieu Functions, Dover N.Y. (1964).

26. McLachlan, N.W.: loc cit, p. 39.

27. McLachlan, N.W.: loc cit, p. 59ff.

28. DeBra, D.B.: Proc. Conf. on Experimental Tests of Gravitational Theories, Caltech, Nov. 1970.

29. Battin, R.H.: Astronautical Guidance, McGraw-Hill, N.Y. (1964).

30. Goldstein, H.: Classical Mechanics, Addison-Wesley, Boston 1965, p. 149.

31. Goldstein, H.: loc cit, p. 159ff.

32. DeBra, D.B.: Proc. Conf. on Experimental Tests of Gravitational Theories, Caltech, Nov. 1970.

33. DeBra, D.B., private communication.

34. Purcell, E.M.: Electricity and Magnetism, McGraw-Hill, N.Y. 1963, p. 352ff.

35. Jackson, J.D.: Classical Electrodynamics, Wiley, NY (1962),p.161.

36. Wilk, L.S.: Pseudodiamagnetic Suspension, Rev. Sci. Instruments, 43, 2, February 1972.

37. Winter, D.L.: Astronautics & Aeronautics, 15, 6(1977) p.54.

38. Rosen, H.A. & Jones, R.: Astronautics & Aeronautics, 15, 6 (1977), p. 48.

39. Weiss, R., private communication.
